



**IMPROVING THE ANISOTROPIC MECHANICAL PROPERTIES
AND MICROSTRUCTURE PRODUCED BY WIRE AND ARC
ADDITIVE MANUFACTURING**



**BACHELOR OF MECHANICAL ENGINEERING TECHNOLOGY
(AUTOMOTIVE TECHNOLOGY) WITH HONOURS**

2023



**Faculty of Mechanical and Manufacturing Engineering
Technology**



**IMPROVING THE ANISOTROPIC MECHANICAL PROPERTIES
AND MICROSTRUCTURE PRODUCED BY WIRE AND ARC
ADDITIVE MANUFACTURING**

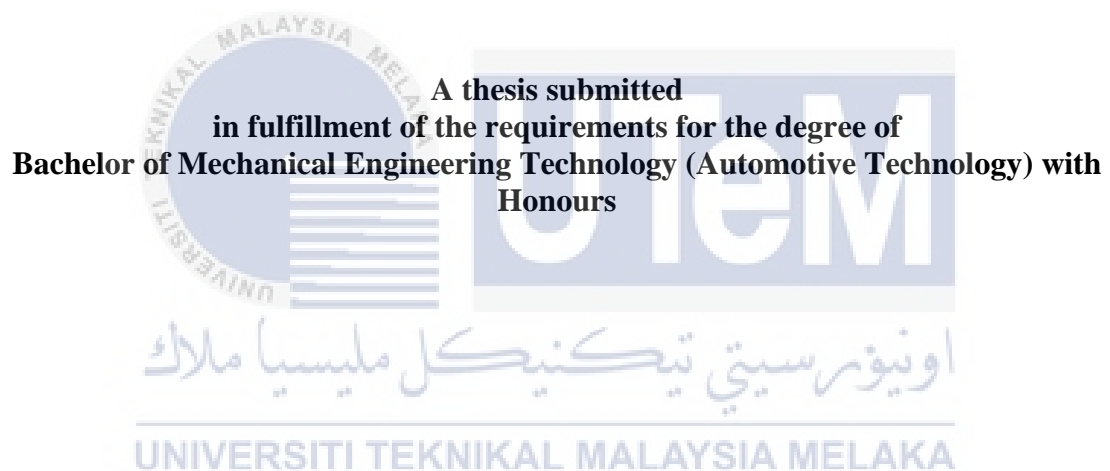
Zarif Ikram Bin Zakir

**BACHELOR OF MECHANICAL ENGINEERING TECHNOLOGY
(AUTOMOTIVE TECHNOLOGY) WITH HONOURS**

2023

**IMPROVING THE ANISOTROPIC MECHANICAL PROPERTIES AND
MICROSTRUCTURE PRODUCED BY WIRE AND ARC ADDITIVE
MANUFACTURING**

ZARIF IKRAM BIN ZAKIR



Faculty of Mechanical and Manufacturing Engineering Technology

UNIVERSITI TEKNIKAL MALAYSIA MELAKA

2023

DECLARATION

I declare that this thesis entitled “Improving The Anisotropic Mechanical Properties And Microstructure Produced By Wire And Arc Additive Manufacturing” is the result of my own research except as cited in the references. The thesis has not been accepted for any degree and is not concurrently submitted in candidature of any other degree.

Signature

:



Name

:

Zarif Ikram Bin Zakir

Date

:

16/06/2023



اونيورسيتي تيكنيكل مليسيا ملاك
UNIVERSITI TEKNIKAL MALAYSIA MELAKA

APPROVAL

I hereby declare that I have checked this thesis and in my opinion, this thesis is adequate in terms of scope and quality for the award of the Bachelor of Mechanical Engineering Technology (Automotive Technology) with Honours.

Signature :



IR. TS. DR. LAILATUL HARINA BINTI PAIJAN
Pensyarah Kanan
Jabatan Teknologi Industri
Fakulti Teknologi Kejuruteraan Mekanikal Dan
Pembuatan (FTKMP)
Universiti Teknikal Malaysia Melaka

Supervisor Name : Ir. Ts. Dr. Lailatul Harina Binti Paijan.

Date : 16/06/2023

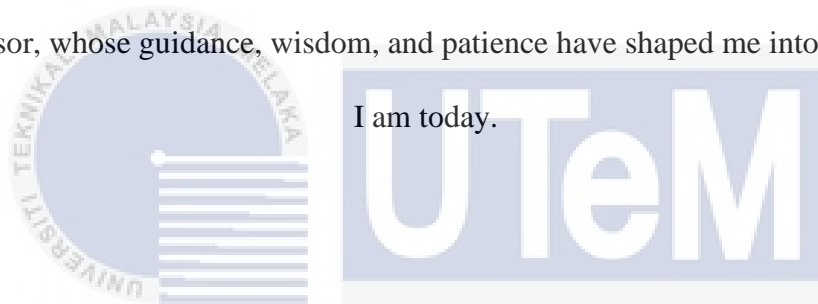
اويور سيتي تيكنيكل مليسيا ملاك

UNIVERSITI TEKNIKAL MALAYSIA MELAKA

DEDICATION

To my family, whose unwavering support and love have been my rock throughout this journey.

To my advisor, whose guidance, wisdom, and patience have shaped me into the researcher I am today.



To my friends, for their constant encouragement, understanding, and for always being there to lift my spirits.

UNIVERSITI TEKNIKAL MALAYSIA MELAKA

And to all those who believe in the power of knowledge and its ability to transform lives, this thesis is dedicated to you.

May this work contribute to the advancement of our collective understanding and inspire future generations of scholars and innovators.

ABSTRACT

Wire Arc Additive Manufacturing (WAAM) represents an advanced and swiftly advancing additive manufacturing method with significant potential for diverse applications. This process entails the incremental deposition of material using an electric arc as the heat source, with a continuous supply of wire serving as the consumable material. This study aims to address the issue in existing research concerning the anisotropy characteristic of Wire and Arc Additive Manufacturing (WAAM) product mainly stainless steel. Therefore, this work focused on to solve the anisotropic characteristic of WAAM sample to reach isotropic characteristic. The optimal welding parameter to make sure the sample reach required thickness which is 8mm are 4m/min wire feed rate, 12.4V voltage and 140A current. This study found that for tensile test, different direction of specimen obtained from both side of certain WAAM sample produced isotropic behaviour while some did not. side B produce a highest result at 694.317MPa compared to side A with 601.292Mpa tensile stress. Impact test found that averagely, side A with highest energy absorbed of 19.88J produce a better result compared to side B with the lowest value is 64.21J. Microstructure analysis found that the microstructure for angled deposition produced better result compared to normal deposition strategy with the top and bottom regions has more congested δ -ferrite compared to γ -austenite and vice versa for middle region.. Based on the finding, the improvement can give benefits to the manufacturer in the industry to use the information in this study to enhance their WAAM to improve the product quality.

اونيورسيتي تيكنيكل مليسيا ملاك

UNIVERSITI TEKNIKAL MALAYSIA MELAKA

ABSTRAK

Wire Arc Additive Manufacturing (WAAM) mewakili kaedah pembuatan aditif yang maju dan berkembang pesat dengan potensi besar untuk aplikasi yang pelbagai. Proses ini memerlukan pemendapan tambahan bahan menggunakan arka elektrik sebagai sumber haba, dengan bekalan wayar berterusan berfungsi sebagai bahan habis pakai. Kajian ini bertujuan untuk menangani isu dalam penyelidikan sedia ada mengenai ciri anisotropi produk Wire and Arc Additive Manufacturing (WAAM) terutamanya keluli tahan karat. Oleh itu, kerja ini memberi tumpuan kepada menyelesaikan ciri anisotropik sampel WAAM untuk mencapai ciri isotropik. Parameter kimpalan optimum untuk memastikan sampel mencapai ketebalan yang diperlukan iaitu 8mm ialah kadar suapan wayar 4m/min, voltan 12.4V dan arus 140A. Kajian ini mendapati bahawa untuk ujian tegangan, arah spesimen yang berbeza yang diperolehi daripada kedua-dua belah sampel WAAM tertentu menghasilkan tingkah laku isotropik manakala ada yang tidak. Sisi B menghasilkan keputusan tertinggi pada 694.317MPa berbanding sisi A dengan tegangan 601.292Mpa. Ujian impak mendapati secara purata sisi A dengan tenaga yang paling tinggi diserap 19.88J menghasilkan keputusan yang lebih baik berbanding sisi B dengan nilai terendah 64.21J. Analisis mikrostruktur mendapati bahawa struktur mikro untuk pemendapan bersudut menghasilkan keputusan yang lebih baik berbanding strategi pemendapan biasa dengan kawasan atas dan bawah mempunyai δ -ferrite yang lebih sesak berbanding γ -austenit dan sebaliknya bagi kawasan tengah.. Berdasarkan dapatan, penambahbaikan boleh memberi manfaat kepada pengilang dalam industri untuk menggunakan maklumat dalam kajian ini untuk meningkatkan kualiti WAAM mereka.

اونيورسيتي تيكنيكل مليسيا ملاك
UNIVERSITI TEKNIKAL MALAYSIA MELAKA

ACKNOWLEDGEMENTS

In the Name of Allah, the Most Gracious, the Most Merciful

First and foremost, I would like to thank and praise Allah the Almighty, my Creator, my Sustainer, for everything I received since the beginning of my life. I would like to extend my appreciation to the Universiti Teknikal Malaysia Melaka (UTeM) for providing the research platform. Thank you also to the Malaysian Ministry of Higher Education (MOHE) for the financial assistance.

My utmost appreciation goes to my main supervisor, Ir. Ts. Dr. Lailatul Harina Binti Paijan, Universiti Teknikal Malaysia Melaka (UTeM) for all his support, advice and inspiration. His constant patience for guiding and providing priceless insights will forever be remembered. Also, to my co-supervisor, En. Hairizal, Universiti Teknikal Malaysia Melaka (UTeM) who constantly supported my journey. My special thanks go to both of them for all the help and support I received from them.

Last but not least, from the bottom of my heart I express gratitude to my fellow PSM members and friends for their encouragement. And I would also like to thank my beloved parents for their endless support, love and prayers. Finally, thank you to all the individual(s) who had provided me with the assistance, support and inspiration to embark on my study.



TABLE OF CONTENTS

	PAGE
DECLARATION	
APPROVAL	
DEDICATION	
ABSTRACT	ii
ACKNOWLEDGEMENTS	iv
TABLE OF CONTENTS	v
LIST OF TABLES	viii
LIST OF FIGURES	ix
LIST OF APPENDICES	xii
1 CHAPTER 1 INTRODUCTION	13
1.1 Background	13
1.2 Problem Statement	14
1.3 Research Objective	15
1.4 Scope of Research	15
2 CHAPTER 2 LITERATURE REVIEW	16
2.1 Introduction	16
2.2 Additive Manufacturing	16
2.3 Wire Arc Additive Manufacturing (WAAM)	17
2.4 History of Wire Arc Additive Manufacturing	18
2.5 Wire and Arc Additive Manufacturing (WAAM) Process and Variants	22
2.5.1 Plasma Arc Welding (PAW)	22
2.5.2 Gas Tungsten Arc Welding (GTAW)	23
2.5.3 Gas Metal Arc Welding (GMAW)	24
2.5.4 Comparison of GMAW and GTAW	24
2.5.5 Cold Metal Transfer (CMT)	25
2.6 WAAM Parameter and Process Planning	25
2.6.1 Steps in Process Planning	26
2.6.2 CAD modelling and 3D slicing	27
2.6.3 Tool Path Generation and Parameters	28
2.6.4 Heat input	30
2.6.5 Welding parameters in WAAM	30
2.6.6 Automatic motion control parameters	32
2.7 Mechanical properties	34
2.8 Isotropy and Anisotropy	35

2.9	Anisotropy of WAAM sample	35
2.10	Stainless Steel	37
2.11	Comparison of research gap	38
2.12	Summary or research gap	39
3	CHAPTER 3 METHODOLOGY	40
3.1	Introduction	40
3.2	Flow Chart	40
3.2.1	Stainless Steel 308LSi	42
3.3	Machine Setup	43
3.3.1	Selection of WAAM Parameter	43
3.3.2	Jig for Substrate	44
3.3.3	Positioner	45
3.3.4	Shielding Gas	46
3.4	Software	47
3.4.1	SolidWorks	48
3.4.2	Cura	48
3.4.3	Repetier	49
3.4.4	3DP	49
3.5	Sample Preparation	50
3.6	Horizontal Band sawing Machine PR-10V.	50
3.6.1	Electrical Discharge Machine (EDM) Wire Cut	52
3.6.2	Milling Machine	56
3.7	Mechanical Properties	57
3.7.1	Tensile Test	58
3.7.2	Charpy Impact Test	59
3.8	Hardness Test	61
3.9	Microstructural Analysis	62
3.9.1	Hot mounting	62
3.9.2	Grinder and polishing machine	63
3.9.3	Optical Microscope	65
3.10	Summary	66
4	CHAPTER 4	68
4.1	Introduction	68
4.2	Tensile Test	68
4.2.1	Result of Tensile Test Specimen	69
4.3	Charpy Impact Test	74
4.3.1	Result of Charpy Impact Test Specimen	74
4.4	Microhardness Test	76
4.5	Microstructural Analysis	78
4.5.1	Top Region	79
4.5.2	Middle Region	80
4.5.3	Bottom Region	81
4.6	Summary	82
5	CHAPTER 5	83
5.1	Conclusion	83

5.2	Recommendation	85
5.3	Project potential	86
REFERENCES		87
APPENDICES		91
Appendix A		91



LIST OF TABLES

TABLE	TITLE	PAGE
Table 2.1	Major areas of study of WAAM technique in the recent past(Derekar, 2018)	21
Table 3.1	Deposited Chemical Composition % of 308LSi Stainless steel	42
Table 3.2	308lsi Stainless Steel Mechanical Properties	42
Table 3.3	ABB Robot Welding Parameter	43
Table 3.4	Side for each sample	55
Table 3.5	Charpy impact test parameters	61
Table 3.6	Micro-Vickers hardness testing parameter	62
Table 3.7	Mounting press machine parameter	63
Table 4.1	Tensile test result	71
Table 4.2	Both side difference for each mechanical properties	72
Table 4.3	Average difference for all mechanical properties	72
Table 4.4	Data for Charpy Impact Test Energy Absorbed	75
Table 4.5	Sample 3 Micro-Vickers Hardness result	77

LIST OF FIGURES

FIGURE	TITLE	PAGE
Figure 2.1	3D printed WAAM hook (Khodabakhshi & Gerlich, 2018)	18
Figure 2.2	History of WAAM (Derekar, 2018)	18
Figure 2.3	Schematic diagram showing superposed deposit of metal (Heilig, 1994).	19
Figure 2.4	Technical drawing showing a thick-walled circular cross-section pressure vessel (Ujiie, 1966).	19
Figure 2.5	Development and complexity of the WAAM process over the years .	20
Figure 2.6	Schematic representation of the wire and arc additive manufacturing (WAAM) process	22
Figure 2.7	Steps in a WAAM system	27
Figure 2.8	(a)Component with basic build direction (b)supports required (c)multidirectional slicing with build direction B1, B2 and B3(Singh et al., 2020)	28
Figure 2.9	Tool Paths for any AM process (a) Raster, (b) Zig-Zag, (c) Contour, (d) Spiral, (e) Hybrid tool paths(Tomar et al., 2022)	29
Figure 2.10	Setup of integrated WAAM system in a CNC gantry	33
Figure 2.11	Robotic arm setup of WAAM used at Cranfield University	34
Figure 2.12	Cutting plan(Hassel & Carstensen, 2020)	36
Figure 3.1	Flowchart	41
Figure 3.2	SS308lsI Stainless Steel LSi	42
Figure 3.3	ABB robot welding produced wall	44
Figure 3.4	Support Jig	45

Figure 3.5	Tilted work table	46
Figure 3.6	Tilted Work Table with substrate clamped	46
Figure 3.7	Shielding gas	47
Figure 3.8	Horizontal Band sawing Machine PR-10V	51
Figure 3.9	Sample after cutting process	51
Figure 3.10	Sodick VZ300L EDM wire-cut machine.	53
Figure 3.11	0.25mm diameter EDM wire	53
Figure 3.12	Sample after wirecut process	54
Figure 3.13	Tensile test specimen dimension according to ASTM E8	54
Figure 3.14	Charpy impact test specimen according to ASTM E23	55
Figure 3.15	FM-16VS Milling Machine	56
Figure 3.16	Milling process	57
Figure 3.17	Tensile and impact specimen after milling.	57
Figure 3.18	Floor Mounted Material Testing System. Instron Model 5585 Capacity 200KN.	58
Figure 3.19	Tensile specimen before and after tensile test	59
Figure 3.20	Charpy Impact Test Machine	60
Figure 3.21	Charpy impact specimen before and after impact test	60
Figure 3.22	Vickers Hardness Tester. Shimadzu HMV-G31.	61
Figure 3.23	Mounting press machine Ecorpes 100	63
Figure 3.24	Grinding and polishing machine	64
Figure 3.25	Grinding and polishing process	65
Figure 3.26	Sample after polishing and grinding	65
Figure 3.27	Nikon Eclipse Lv100 Microscope Machine.	66

Figure 3.28	etching solution for stainless steel	66
Figure 3.29	Microstructure sample after etching	66
Figure 4.1	Tensile Test Specimen	69
Figure 4.2	Sample 1 tensile test result	70
Figure 4.3	Sample 2 tensile test result	70
Figure 4.4	Sample 3 tensile test result	70
Figure 4.5	Sample 4 tensile test result	71
Figure 4.6	Tensile stress at maximum load	73
Figure 4.7	Charpy impact test specimen	74
Figure 4.8	Charpy Impact Test result graph	75
Figure 4.9	Micro-Vickers Hardness value graph	78
Figure 4.10	a)top region of sample b)microstructure under 50x magnification c)microstructure under 100x magnification d)layer boundary under 50x magnification e)layer boundary under 100x magnification	79
Figure 4.11	a)middle region of sample b)microstructure under 50x magnification c)microstructure under 100x magnification d)layer boundary under 50x magnification e)layer boundary under 100x magnification	80
Figure 4.12	a)bottom region of sample b)microstructure under 50x magnification c)microstructure under 100x magnification d)layer boundary under 50x magnification e)layer boundary under 100x magnification	81

LIST OF APPENDICES

APPENDIX	TITLE	PAGE
APPENDIX A	Gant Chart	89



1 CHAPTER 1

INTRODUCTION

1.1 Background

Additive manufacturing, commonly known as 3D printing, has revolutionized the manufacturing industry by enabling the creation of complex and customized objects with ease. One such technique that has gained significant attention is Wire Arc Additive Manufacturing (WAAM). WAAM utilizes an electric arc as a heat source to melt and deposit metal wire layer by layer, gradually building up a three-dimensional object. This process offers numerous advantages, including cost-effectiveness, reduced material waste, and the ability to produce large-scale components.

Over the years, a multitude of additive manufacturing technologies has emerged, each with its unique capabilities and materials. From stereolithography and selective laser sintering to fused deposition modeling and direct metal laser sintering, these technologies have revolutionized industries such as aerospace, automotive, medical, and more.

Throughout the years, researchers and engineers have dedicated their efforts to refining the process parameters and expanding the range of materials that can be used in WAAM. The ability to deposit metal layer by layer using electric arc welding techniques has enabled the production of complex and customized metal parts with reduced material waste and cost-effectiveness.

With increasing years and researches come also increments of wide branch of issue that need to be addressed. One of the issues were the anisotropic behavior of sample fabricated by the WAAM. Anisotropy in a simple explanation can be describe as direction-

dependent. In other word, anisotropy is a characteristic of having a physical property which has a different value when measured in different directions. In this case, the sample fabricated by WAAM produced different result in different kind of measurement such as tensile strength, microstructure and such.

Variety of material has been included in these studies as WAAM is a versatile process that can work with a wide range of materials. The choice of material depends on the specific application requirements, including mechanical properties, chemical compatibility, and desired end-use characteristics. Some commonly used materials in WAAM are metal such as steel, aluminum, titanium, nickel-based alloys and copper. Other commonly used material is composite such as metal matrix composites (MMCs), polymer matrix composites (PMCs). Some also use ceramics and refractory metals such as tungsten and molybdenum for its ability of high-temperature resistance and wear resistance.

1.2 Problem Statement

WAAM open a lot of doors of study to be done on its matter from process optimization, material characterization, surface finishing and post-processing and many more as the topic dive really deep into additive manufacturing. Thus, a lot of research has been done on the matters to study about thus topic

. One of the most notable is (Sun et al., 2020). the outcomes of experimental assessments conducted on low-carbon high-strength steel produced through Wire Arc Additive Manufacturing (WAAM) indicate the anisotropic behavior on the WAAM fabricated sample. 3D reconstructions have revealed that the cross-sectional area of tensile specimens exhibits variations in terms of grain and layer boundary orientation across different directions(Robert & Brown, 2004). These factors could have a substantial impact on the mechanical properties, potentially resulting in anisotropy.

To address the issue, our goal is to attain isotropic properties. Isotropic materials are the preferred option due to their uniform characteristics in all directions, a key factor for ensuring the reliability of structures and products. Isotropy streamlines the prediction of material behavior, aiding in the design of components and structures that maintain consistent performance in various scenarios. Moreover, it simplifies the design and manufacturing processes by eliminating the necessity to account for direction-dependent properties, typically resulting in more efficient utilization of materials and resources in real-world engineering applications.

Approaching the study of this issue will benefit the industry and manufacturer as they can use and include this study for their application in producing a material or product using WAAM.

1.3 Research Objective

- a) To fabricate WAAM structure with the deposition at an angled surface using robotic welding.
- b) To study the mechanical properties of WAAM product for charpy impact test and tensile test.
- c) To analyze the microstructure of the WAAM fabricated product.
- d) To reach isotropic characteristic on the produced WAAM deposited wall.

1.4 Scope of Research

The scope of this research are as follows:

- To produce WAAM product on an angled surfaced.
- To evaluate physical test which is the tensile test and impact test.
- To study the microstructure of the WAAM fabricated product using Optical Microscopy(OM).

2 CHAPTER 2

LITERATURE REVIEW

2.1 Introduction

In this chapter, a comprehensive literature review was undertaken to acquire knowledge and enhance the necessary skills for the successful completion of the research. The primary sources consulted for this study included a wide range of materials, such as internet resources, magazines, journals, and articles that were relevant to the research topic. The findings obtained from this review encompass various aspects, including an exploration of different types of WAAM (Wire Arc Additive Manufacturing) process parameters, the analysis will be conducted with various of test and analysis, and the investigation into the welding concept using SS308LSI stainless steel. This section presents the valuable insights gained from these studies, shedding light on the intricacies of the topic at hand and providing a solid foundation for the research project.

2.2 Additive Manufacturing

Additive manufacturing (AM), also known as additive layer manufacturing (ALM), refers to the industrial method of producing three-dimensional objects using 3D printing. This computer-controlled process involves depositing materials, typically in layers, to create the desired objects. By utilizing additive manufacturing, 3D objects scanners, and computer aided design (CAD) allow the production of objects characterized by precise geometric shapes. This cutting-edge method builds things layer by layer, much like 3D printing.. This stands in contrast to conventional manufacturing methods that often involve the removal of excess material through machining or other techniques. There exist several

distinct processes in additive manufacturing (AM), each adhering to its own set of standards. These processes encompass Directed Energy Deposition-Arc (DED-arc) is the new name for Binder Jetting, Directed Energy Deposition, Material Extrusion, Powder Bed Fusion, Sheet Lamination, Vat Polymerization, and Wire Arc Additive Manufacturing.(Tomar et al., 2022).

2.3 Wire Arc Additive Manufacturing (WAAM)

The first application of additive manufacturing (AM) was made possible by 3D Systems' introduction of stereolithography (SL). SL uses a laser to solidify thin layers of an ultraviolet (UV) light-sensitive liquid polymer(Wohlert & Gornet, 2012). The novel technique of AM, which involves the step-by-step deposition of materials to build or print three-dimensional parts, has become a significant catalyst for the fourth industrial revolution and has established itself as a mainstream manufacturing process (Gross & Bertoldi, 2019). Unlike traditional methods, with additive manufacturing (AM), components can be produced directly from computer-aided design (CAD) models, doing away with the need for expensive fixtures or assembly for different parts. This ability enables the one-step manufacturing of components with complex profiles(Huang et al., 2013). AM technology has been widely adopted by industries like automotive, aviation, energy, and healthcare that demand innovative engineering applications. Figure 2.1 shows some parts fabricated using wire arc additive manufacturing (WAAM) (Khodabakhshi & Gerlich, 2018). The layer-by-layer approach of material deposition in AM has expanded the options for part fabrication, offering alternatives to conventional methods such as forming, casting, powder metallurgy, and welding (Liu et al., 2019). While minimizing production time and material consumption is the main goal of additive manufacturing (AM)

processes, addressing performance and structural quality issues is the main challenge facing AM technology (DebRoy et al., 2018).



Figure 2.13D printed WAAM hook (Khodabakhshi & Gerlich, 2018)

2.4 History of Wire Arc Additive Manufacturing

Although the term "near net shape manufacturing through welding" has become widely used in the context of additive manufacturing (AM) in the last fifteen years, the idea behind it dates back nearly a century. Shape welding (SW), shape melting (SM), rapid prototyping (RP), solid freeform fabrication (SFF), shape metal deposition (SMD), and 3D welding are some of the modern welding techniques that inventors have used to create various shapes as a result of advancements in welding technology. From a more comprehensive historical standpoint, the development of WAAM can be categorized into three distinct periods, as illustrated in Figure 2.2.

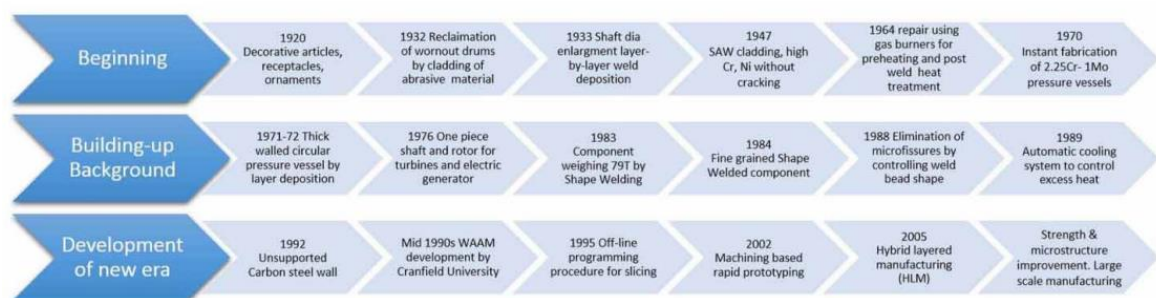


Figure 2.2History of WAAM (Derekar, 2018)

As early as 1920, Baker(Heilig, 1994) filed a patent for the formation of a "superposed deposit of metal" using a manipulated helical path of a fusible electrode to create an ornament as shown in Figure 2.3. Following this creative patent, Shockey (Shockey, 1930) submitted a second patent detailing the application of welding for cladding, with the best results coming from overlapping beads with recommended overlap.. Ujiie (Ujiie, 1966) showed how a circular cross-sectional pressure vessel could be created using only the progressive deposition of weld metal. as shown in Figure 2.4. Additionally, Ujiie talked about the inner and outer layers of the formed part's machining. In the subsequent year, Ujiie (Ujie & Montanye, 1973) developed a three-wire electrode gas metal arc welding (MAG/MIG) technique with an emphasis on deposition rate.



Figure 2.3 Schematic diagram showing superposed deposit of metal (Heilig, 1994).

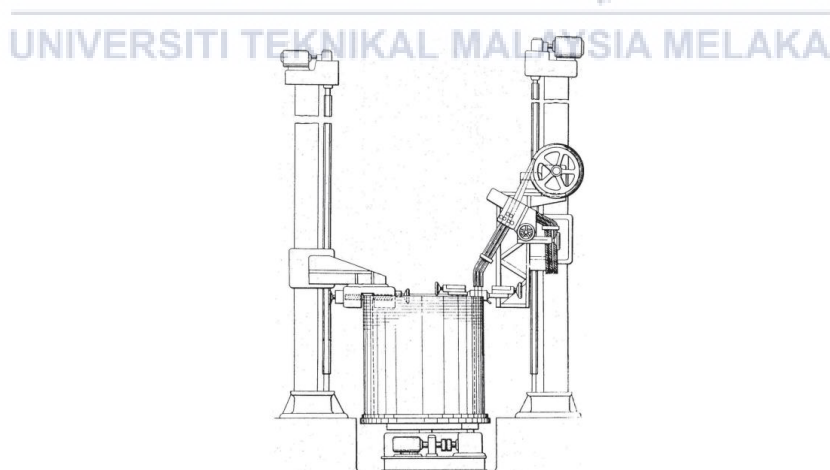


Figure 2.4 Technical drawing showing a thick-walled circular cross-section pressure vessel (Ujiie, 1966).

Computer technology's introduction into the manufacturing sector strengthened and revolutionized 3D welding. Dickens et al. (Dickens et al., 1992) employed robotic GMAW

technology and online point-to-point programming to create an unsupported carbon steel wall layer by layer. Ribeiro and Norrish (Ribeiro, 1996) created an offline monitoring system that made it possible to slice a computer-aided design model and make it easier to deposit weld metal in the desired format layer by layer. Zhang et al. (Zhang et al., 2002) successfully used the Initial Graphics Exchange Specification (IGES) format to accomplish component slicing into multiple layers. Large shapes like pressure vessels could be manufactured by inventors thanks to the intricacy of WAAM, which followed a trend of process simplification in terms of operation, material handling, formulation, and conceptualization. The technique had to be reinvented when computer-controlled systems were introduced in manufacturing because they were very different from conventional manual and machine-controlled processes. Although sophisticated testing methods help create safer structures, fulfilling the test requirements adds another level of complexity. The development of WAAM and the increasing complexity of the process are visually represented in Figure 2.5.

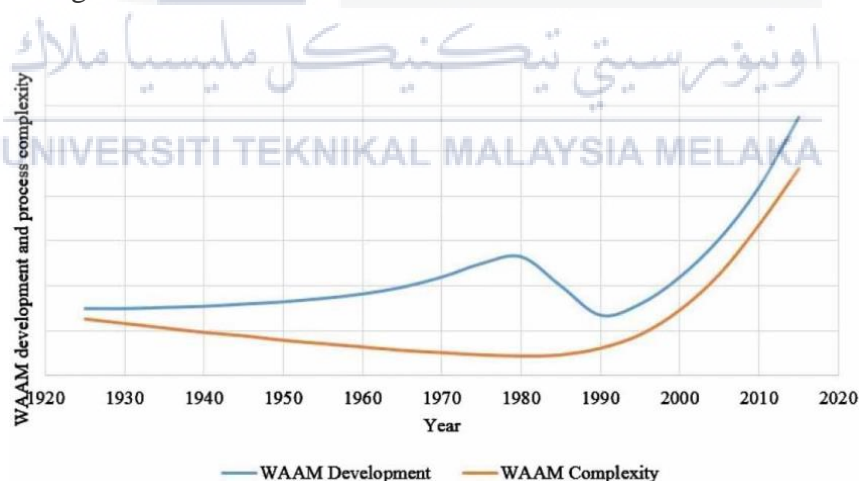


Figure 2.5 Development and complexity of the WAAM process over the years .

Back in the 1990s, Rolls-Royce and Cranfield University indicated interest in utilizing the SMD process to produce aero engine parts made of Inconel 718 and Ti-6Al-4V alloys. Consequently, a wide range of theoretical and applied modeling techniques have

been used to investigate the developing field of WAAM. Some notable studies in recent years are summarized in Table 2.1 as researched by K. S. Derekar (Derekar, 2018). Researchers thoroughly study the behavior of single-bead, multi-layer (open loop) structures in order to understand the principles of WAAM. They concentrate on elements like the forming appearance, design, development, and distribution of residual stress.

Table 2.1 Major areas of study of WAAM technique in the recent past(Derekar, 2018)

Area of study	Year	Specific area of study	Material/filler wire
Design	2011	• Cross structures	Steel
		• Root path determination	Steel (ER70S-6), Aluminium (4043)
	2014	• Inclined wall preparation	
		• Preparation of horizontal wall and closed shape	Mild steel, Titanium (Ti-6Al-4V)
	2015	• Deposition patterns	Mild steel
	2016	• Cross-structures	-
		• Tool path planning	Steel (ER70S-6)
Process variation	2005	• Hybrid manufacturing	Steel
	2014	• T-crossing	Steel (ER70S-6)
		• Adaptive path generation	Steel (ER70S-6)
	2016	• Hybrid manufacturing using milling	Steel (ER70S-6) & Steel ER110S-6
		• Twin wire GMAW	Steel (H08Mn2Si)
	2017	• Double-electrode GMAW	Steel (ER70S-6) & Steel ER110S-G
		• Dissimilar twin wire deposition (functionally gradient part formation)	Steel (H08Mn2Si)
• Double-electrode GMAW		Aluminium 2325	
• Hybrid manufacturing with milling		Steel (ER70S-6)	
2018	• Hybrid manufacturing	Aluminium ER2319 and ER5087	
	• Dissimilar twin wire GTAW deposition		
Residual stress	2007	• Finite elemental structural study	Steel (Simulation)
	2011	• Computer simulation	Steel
	2015	• Distortion control	Steel, Aluminium and Titanium (Ti-6Al-4V)
		• Computational model for twin wire AM	Steel (ER70S-6), Steel (ER70S-6), Titanium (Ti-6Al-4V)
Forming appearance	2014	• Bulk deformation	
		• Microstructure	
	2015	• Passive vision sensor system	Steel
		• Parametric study	Steel
	2016	• Bead overlapping factor	Steel
• Double electrode GMAW parametric study		Steel (H08Mn2Si)	
• Minimum angle and curvature of radius		Aluminium 5A06	
Interlayer-rolling and its effect on microstructure, mechanical properties and residual stresses	2017	• Control of arc start and end	Steel
		• Inclined wall structure	Steel (H08Mn2Si)
	2013	• Effect of different profiled rollers	Steel (ER70S-6)
		• Grain structure refining	Titanium (Ti-6Al-4V)
	2014	• Mechanical properties	
		• Distortion	Titanium (Ti-6Al-4V)
	2016	• Refined microstructure	Titanium (Ti-6Al-4V)
• Reduction of residual stresses		Titanium (Ti-6Al-4V)	
• Controlling residual stresses		Aluminium (ER2319)	
• Precipitation hardenable alloy		Aluminium (ER2319 and 5087)	
2017	• Porosity formation behaviour in work and precipitation hardenable alloy		
	• β grain refinement in Ti-6Al-4V	Titanium (Ti-6Al-4V)	
Cold metal transfer (CMT)	2010	• Al-Mg4.5Mn alloy	Aluminium (ER5087)
		• Application for Ti-6Al-4V	Titanium (Ti-6Al-4V)
	2014	• Parametric study with AISI5	Aluminium (AISI5)
		• Variants of CMT technique	Aluminium (2319)
Fatigue failure and toughness	2016	• Effect on porosity	Aluminium (ER2319)
		• Variants of CMT technique	Aluminium (ER2319)
	2017	• Wall and block structure	Aluminium (ER2319)
		• Varying polarity and microstructural considerations	Al-6Mg
2013	• Fatigue life	Titanium (Ti-6Al-4V)	
	• Fatigue crack growth propagation	Titanium (Ti-6Al-4V)	
	• Fatigue crack path selection	Titanium (Ti-6Al-4V)	
2017	• Fatigue crack growth rate	Titanium (Ti-6Al-4V)	

2.5 Wire and Arc Additive Manufacturing (WAAM) Process and Variants

Wire Arc Additive Manufacturing (WAAM) is classified as direct energy deposition in ASTM F2792-12a. It is distinguished by the use of wire as the feedstock material and an electric arc as a heat source. Figure 2.6 provides a schematic representation of the WAAM process. The basic ideas of automated welding processes, such as gas metal arc welding (GMAW), plasma arc welding (PAW), and gas tungsten arc welding (GTAW), are incorporated into WAAM.

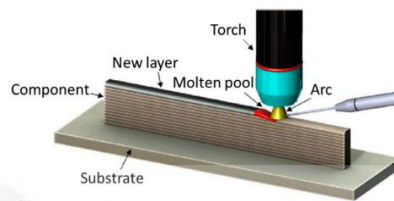


Figure 2.6 Schematic representation of the wire and arc additive manufacturing (WAAM) process

2.5.1 Plasma Arc Welding (PAW)

The arc welding technique known as plasma arc welding (PAW) is comparable to gas tungsten arc welding (GTAW). In PAW, a workpiece and an electrode—typically made of sintered tungsten, though other materials can be utilized as well—create an electric arc. The main way that PAW differs from GTAW is that the electrode is placed inside the torch body, which separates the shielding gas envelope from the plasma arc. After that, the plasma is forced through a slender copper nozzle, which narrows the arc and causes the plasma to escape the orifice at high speeds that are almost as fast as sound and at a temperature that is at least 28,000 °C (50,000 °F).

An arc plasma is a temporary state of a gas. The gas becomes conductive and ionizes when an electric current flows through it. In the ionized state, the gas molecules break into electrons (–) and cations (+), resulting in a mixture of ions, electrons, and highly excited atoms. Double and triple degrees of ionization can be used to increase the level of ionization

from 1% to more than 100%. When electrons are dragged out of their orbits, these states form.

The electrical power used to create the arc plasma determines the temperature of the plasma jet and, in turn, its energy. The temperature in a plasma jet torch is usually about 28,000 °C (50,400 °F), which is much higher than the 5,500 °C (9,930 °F) that is found in typical electric welding arcs.

2.5.2 Gas Tungsten Arc Welding (GTAW)

TIG (tungsten inert gas) welding, commonly referred to as gas tungsten arc welding (GTAW), is an arc welding technique that produces the weld using a non-consumable tungsten electrode. An inert shielding gas, usually argon or helium, protects the electrode and the weld area from oxidation and airborne contaminants. Even though filler metal is frequently used, some welds referred to as autogenous or fusion welds can be made without it. The process is called heliarc welding when helium is used.

An arc is created when electrical energy from a constant-current welding power supply flows through a plasma, which is a highly ionized gas and metal vapor column. The most common uses for TIG welding are the joining of thin stainless-steel sections and non-ferrous metals such as copper alloys, magnesium, and aluminum. Compared to other methods like gas metal arc welding (GMAW) and shielded metal arc welding (SMAW), this process gives the operator more control over the weld, producing stronger and better welds. TIG welding is slower than many other welding techniques, but it is also comparatively more complex and difficult to learn. A similar technique known as plasma arc welding uses a marginally different welding torch to create a more concentrated welding arc, which frequently makes automation possible.

2.5.3 Gas Metal Arc Welding (GMAW)

Gas metal arc welding (GMAW), sometimes referred to as metal inert gas (MIG) or metal active gas (MAG) welding, is a type of welding in which the workpiece metal(s) and a consumable MIG wire electrode create an electric arc. The heat produced by this arc causes the metal(s) in the workpiece to melt and fuse together. A shielding gas is fed through the welding gun with the wire electrode to prevent contamination from the atmosphere.

GMAW can be run automatically or semi-automatically. Although alternating current and constant current systems can also be used, constant voltage, direct current systems are the most often used power source for GMAW. In GMAW, there are four main ways to transfer metal: globular, spray, short-circuiting, and pulsed-spray. Every technique has particular qualities, as well as particular benefits and drawbacks.

2.5.4 Comparison of GMAW and GTAW

Both gas metal arc welding and gas tungsten arc welding possess similar concepts that may have the same effect on the produced sample based on their parameters. Studies by Ramazan Yilmaz and Huseyin Uzun (YILMAZ & HUSEYIN UZUN, 2002), higher tensile strength and toughness values were obtained from the weld of GTAW compared to GMAW. But the similarities of both arc welding are with increased current will have the same effect on the mechanical properties of the sample produced. Elevated welding currents contribute to increased heat input, raising the temperature of both the welding pool and the substrate. This, in turn, enhances the fluidity of the deposited material. It can be observed that higher welding currents lead to wider welds, greater penetration, and increased dilution (Tomaz et al., 2021). By increasing the welding current to 90, 150, and 210 A, the depth of penetration increases. The welding current plays a crucial role in determining the penetration level.

Additionally, the penetration is influenced by other factors such as welding speed and arc voltage(Ibrahim et al., 2012).

One often used method in Wire Arc Additive Manufacturing (WAAM) processes is Gas Metal Arc Welding (GMAW). It increases productivity and efficiency by offering a deposition rate that is two to three times higher than that of gas tungsten arc welding (GTAW)(Tomar et al., 2022). Furthermore, The efficiency of GMAW-based additive manufacturing (AM) is highlighted by the fact that it exhibits nearly twice the deposition rate when compared to GTAW- and PAW-based AM(Tomar et al., 2022).

2.5.5 Cold Metal Transfer (CMT)

One type of welding technology used in Wire Arc Additive Manufacturing (WAAM) systems is called Cold Metal Transfer (CMT). Arc energy is used as the heat source in WAAM, a directed energy deposition (DED) technique for additive manufacturing. (Novelino et al., 2022) in his study use a 3-axes deposition setup and a Fronius TransPuls Synergic 5000 CMT power source are used in the CMT-based WAAM system.

Precise metal deposition is made possible by the combination of WAAM and CMT power sources, (Novelino et al., 2022) have looked into how wall structures are affected by the WAAM-CMT deposition parameters. The behavior of CMT wire in the WAAM process has been studied through experimental and numerical research, which has yielded important insights into its use(Yuan et al., 2022).

2.6 WAAM Parameter and Process Planning

Typically, wire arc additive manufacturing (WAAM) produces work components that are near-net shape, but they may have a surface finish that falls below the desired standards. Therefore, additional machining is often required to achieve the final component specifications. Nonetheless, the utilization of computer-aided process planning can

mitigate this constraint associated with WAAM strategies. One important step in WAAM that affects the final output quality is process scheduling. The creation of 2.5 D layers, the identification of the deposition paths for these layers, and the setting of welding parameters like wire-feed rate, travel speed, and stick-out—all of which are influenced by the deposition paths and managed by a computer-controlled robotic arm—are some of the crucial steps in the automated process planning for WAAM. Creating a clear strategy is crucial to using the WAAM technique and ensuring best practices in product manufacturing. Process planning steps including slicing and tool path planning are involved in this (Singh et al., 2020).

2.6.1 Steps in Process Planning

A wire arc additive manufacturing (WAAM) system's process planning involves a number of arrangements, including CAD modeling, 2D route planning, 3D slicing techniques, weld bead geometry and related modeling, weld parameters, coding, and post-processing, as depicted in Figure 2.7. Slicing ready-made 3D CAD models into 2D layers is the first step. Then, for every sliced layer, suitable deposition paths are created during the 2D route planning stage. The optimal bead geometries along these paths are identified after the paths are constructed. The arrangement of variables is aided by bead modeling, and the best welding parameters in relation to the intended bead geometry are determined. The robot code generation module then transfers the deposition route and the chosen welding parameters to a coordinated robot code file. Lastly, the welding technique is employed by the automated robotic arm to deposit a near-net shape. Usually, extra post-processing steps are needed to produce a finished product with exact dimensional accuracy. Achieving defect-free structures requires careful 2D path planning and the selection of WAAM weld parameters.

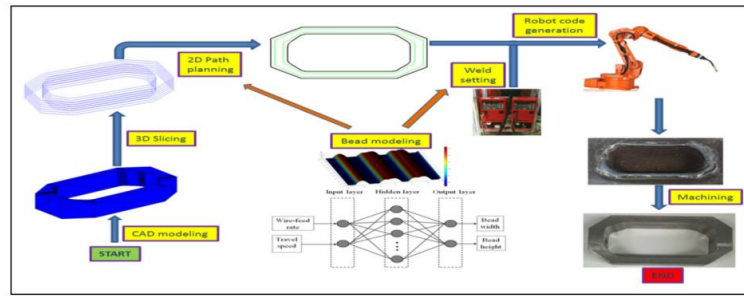


Figure 2.7 Steps in a WAAM system

2.6.2 CAD modelling and 3D slicing

In additive manufacturing (AM), a computer-aided design (CAD) model of the component is used. This model can be created in advance or acquired through reverse engineering. The widely used CAD template in additive manufacturing, representing 3D CAD models, is the standard 'STL' format. The majority of current additive manufacturing processes split the 3D CAD model into several 2D layers with either constant or variable thickness.

Currently, AM machines primarily employ the unidirectional slicing technique due to its simplicity. However, this method is typically limited to producing complex shapes because it necessitates the use of support structures for overhanging parts. To overcome this limitation, the multi-directional slicing (MDS) technique, as illustrated in Figure 2.8, has been introduced. MDS enhances the capabilities of AM and reduces the need for supports. Nevertheless, implementing MDS is still constrained by the requirement for AM machines capable of depositing material in different directions (Singh et al., 2020). Additionally, the complexity and lack of adaptability of MDS algorithms present challenges. This highlights the need for a complete robotic configuration for wire arc additive manufacturing (WAAM) deposition.

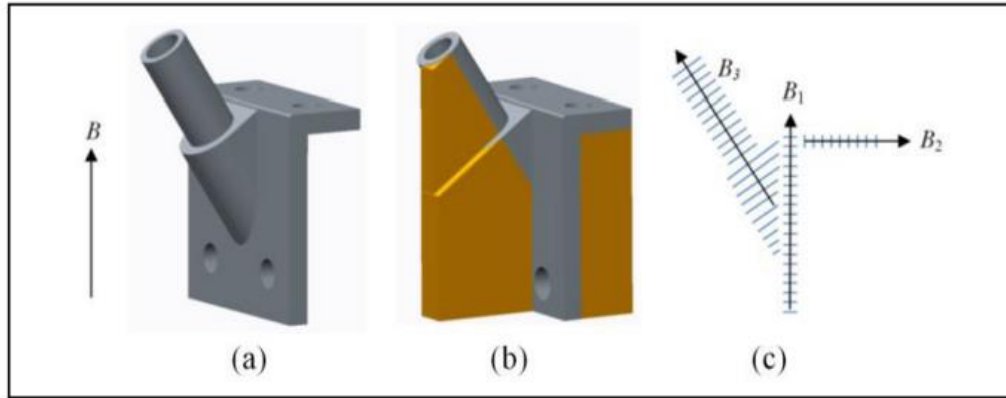


Figure 2.8(a)Component with basic build direction (b)supports required (c)multidirectional slicing with build direction B_1 , B_2 and B_3 (Singh et al., 2020)

One of many software that has been intergrated into WAAM as a slicing component is Ultimaker CURA Slicer. (Navarro et al., 2022) has used Cura Slicer in his study and has produced a great result in several aspect due to its simple and friendly user display and compatible with various type of 3D printing including WAAM.

2.6.3 Tool Path Generation and Parameters

One of the most important steps in wire arc additive manufacturing (WAAM) is to improve the route planning method. The route planning arrangements for AM steps involving approximate deposits are impacted by mathematical uncertainty. Furthermore, the direction of the deposition path may have an impact on the characteristics of the material that is deposited. Different types of deposition paths have been produced by various tool path generation techniques that have been reported in the literature.

Raster tool path that produces the raster filling path, as shown in Figure 2.9(a), is based on projecting the planar beam along a single line. This method uses numerous scan lines with small widths to fill 2-dimensional regions. It is commonly used in AM due to its simplicity and is suitable for arbitrary boundaries.

Zig-zag tool path that produce the zig-zag approach, depicted in Figure 2.9(b), is similar to the raster path but combines separate parallel lines into a single continuous pass,

reducing the number of tool path passes. Both the raster and zig-zag methodologies have poor outer boundary accuracy due to discretization errors when edges do not align with the tool's motion direction.

Contour tool path that produces the contour path, shown in Figure 2.9(c), follows the outer boundary of the deposition pattern, resolving the outer boundary issues associated with raster and zig-zag tool path planning. Inner fillings are done simultaneously based on the outer boundary structure.

Spiral tool path that produces the spiral tool path, illustrated in Figure 2.9(d), is widely used in machining, such as pocket milling, but can also be applied to AM processes. This method can overcome the limitations of the zig-zag tool path but is suitable for specific geometrical models only.

Hybrid tool path that produces the hybrid tool path planning, as depicted in Figure 2.9(e), combines several promising features from different approaches and is well-suited for AM processes. A blend of contour and zig-zag tool paths is typically used to achieve both mathematical precision and efficient manufacturing. There are various ways to implement hybrid tool path planning, such as using zig-zag for inner filling to enhance performance and contour for the product boundary to improve surface finish.

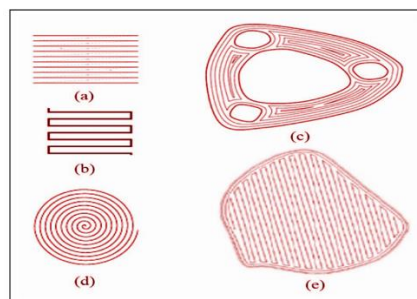


Figure 2.9 Tool Paths for any AM process (a) Raster, (b) Zig-Zag, (c) Contour, (d) Spiral, (e) Hybrid tool paths (Tomar et al., 2022)

Overall, the hybrid tool path (a combination of contour and zig-zag paths) is considered advantageous for WAAM.

To enhance surface quality and minimize distortion, a special pause and run method is applied. After depositing a single bead, a short pause of a few seconds is maintained before the next layer deposition. This pause allows the previous layer's weld beads to settle, resulting in improved surface uniformity and reduced warping. The pause also allows the layer to partially harden, limiting heat absorption by the underlying layers and reducing distortion in the outer surface's geometrical tolerance(Jafari et al., 2021).

2.6.4 Heat input

The effect of heat input is a significant component in Wire Arc Additive Manufacturing (WAAM). Heat input affects the thermal gradient, nucleation rate, and grain growth rate in addition to the mechanical properties and surface quality of parts made using WAAM(Zeng et al., 2021). Electrical energy is converted into heat during the GMAW-WAAM process, melting base metal and filler material. The properties of the arc have a major impact on how much heat is input during this process(Zeng et al., 2021).

Controlling heat input in WAAM is important because it directly affects the final quality and properties of the fabricated components, as research has shown. The linear energy density, which expresses heat input, is an important factor to consider when comparing different WAAM techniques. There are differences between technologies like plasma arc welding (PAW) and gas metal arc welding (GMAW)(Veiga et al., 2022).

2.6.5 Welding parameters in WAAM

For wire arc additive manufacturing (WAAM), four key welding process parameters need to be carefully chosen and monitored in order to identify the specific materials needed. The wire electrode extension, welding voltage, welding speed, wire feed speed, and welding current are some of these parameters. When combined, these variables have a direct impact on the welding characteristics by modifying the process's heat input. With the help of the

welding speed (N), welding current (I), and arc voltage (V), one can determine the heat input rate or arc energy (in J/mm) as shown in .

$$\text{Heat Input} = \frac{V \times I \times 60}{N} \text{ (J/mm)} \quad (2.1)$$

Among these variables, welding current is essential for regulating the arc welding process's weld geometry, fusion depth, and rate of electrode burn off. The speed of wire feed has a direct impact on welding current. A higher welding current causes the weld to penetrate deeper. A stronger welded joint result from deeper penetration.

The electrical potential difference between the welding wire tip and the workpiece or weld pool is referred to as arc voltage. It establishes the reinforcement of the weld and the condition of the fusion zone. The ideal arc voltage is reached at the maximum penetration depth.

Throughout the process, weld penetration and bead size are influenced by weld speed, or the arc's travel speed. Increased travel speed lessens the deposit of metal. Consequently, in order to increase the thickness of the deposited material, the travel speed must be decreased. The right amount of control over the welding speed is necessary for a given material thickness and joint structure.

The distance between the contact tip and the wire tip's end, where the arc is produced, is referred to as wire extension. Excessive weld beads and poor shape with low penetration can be the outcome of a long extension. In general, it is maintained as steady as feasible. These are important adjustments, and keeping track of their values while welding promotes reproducibility.

2.6.6 Automatic motion control parameters

Automatic motion control parameters in the context of Wire Arc Additive Manufacturing (WAAM) usually refers to the automated control settings that specify the motion and positioning of the robotic or gantry system during the additive manufacturing process. In order to achieve accurate and consistent layer deposition in WAAM, these parameters are essential.

The efficacy, accuracy, and repeatability of the WAAM process are enhanced by these automated motion control parameters, guaranteeing reliable and superior additive manufacturing outcomes. These parameters are frequently adjusted by researchers and engineers in accordance with the particular material, geometry, and application requirements.

2.6.6.1 Gantry

In additive manufacturing (AM) processes, such as 3D printing and other 3-axis CNC machines, conventional gantry systems are frequently used. These systems allow for the establishment of a full wire arc additive manufacturing (WAAM) setup, with the welding torch taking the place of the fixed tool, as depicted in Figure 2.10. A locally available PC framework controls the vertical movement of the print bed and the movement of the welding torch along the flat plane.

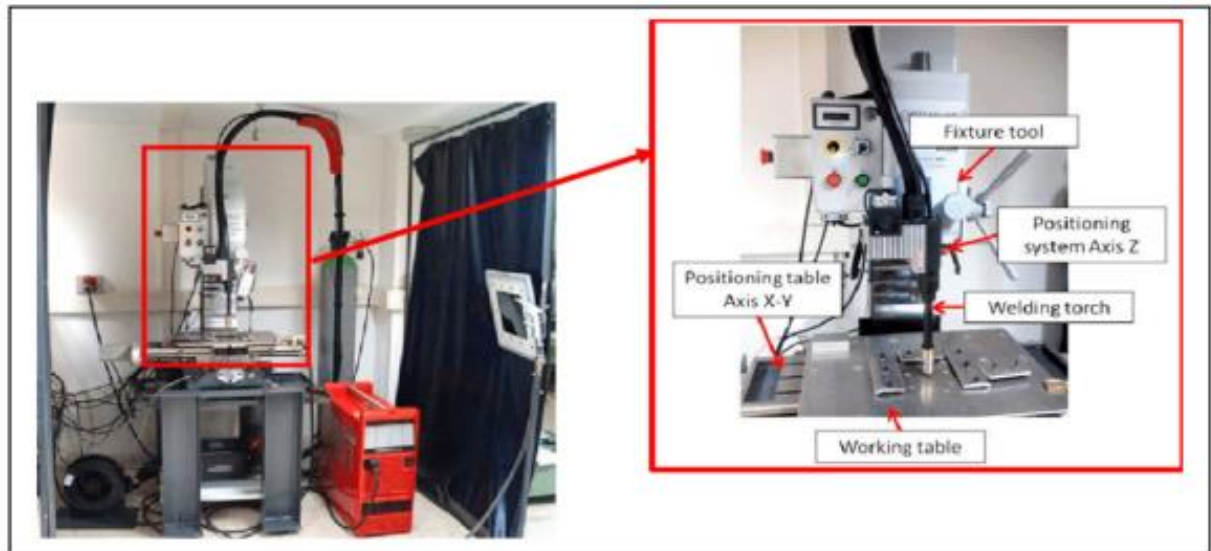


Figure 2.10 Setup of integrated WAAM system in a CNC gantry

2.6.6.2 Robot manipulator

But a significant problem with these three-dimensional structures is the melt pool wire's vertical motion, which keeps melting and leaving behind beads at the bottom of each layer. The simplicity of these structures often leads to vibration issues, causing instability in the weld pool. To address this, new computer programming and steps are required to control the arc and regulate the accumulation of weld beads. As a result, robotic arm setups have been utilized for WAAM experiments. Figure 2.11 illustrates a full cold metal transfer setup with a robotic arm integrated for WAAM.

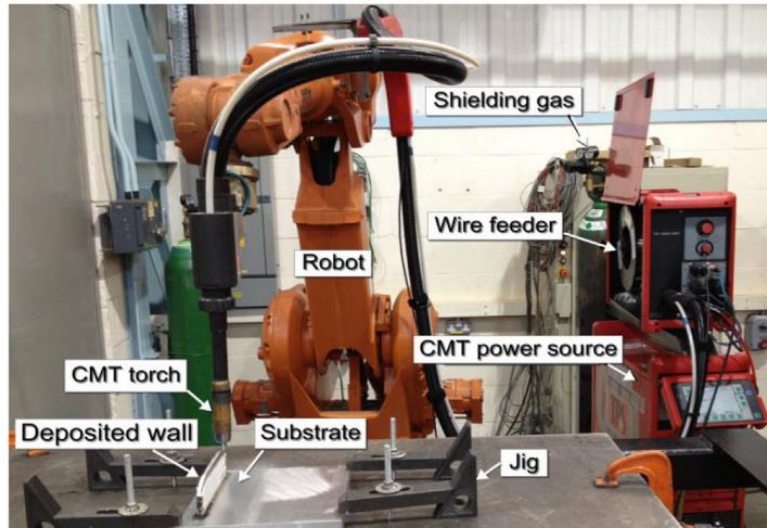


Figure 2.11 Robotic arm setup of WAAM used at Cranfield University

For WAAM setups, the robotic wire feed system has various benefits over the standard gantry system. Weld bead deposition is improved with robotic assistance and stair-step effects are minimized. This is due to the robotic arm's ability to manipulate the metal in all six directions, which improves control and accuracy.

2.7 Mechanical properties

Mechanical properties in Wire-Arc Additive Manufacturing (WAAM) are assessed through various testing methods to understand the performance of materials produced by this additive manufacturing technique. Tensile tests, Charpy impact tests, hardness analysis, and microstructure examinations are commonly conducted to evaluate key mechanical characteristics.

One of it is tensile tests and charpy impact tests. Tensile tests are employed to measure the material's tensile strength, yield strength, and elongation. Charpy impact tests assess the impact toughness and resilience of the material under dynamic loading conditions. On the other hand, hardness analysis provides insights into the material's resistance to indentation or scratching while Microstructure analysis helps understand the internal structure of the material, identifying any defects or irregularities.

2.8 Isotropy and Anisotropy

In physics, material science, and geology, among other disciplines, the term "anisotropy" is used to characterize a quality that depends on direction or displays distinct features along multiple axes or directions. Stated differently, anisotropy is the absence of symmetry or homogeneity in a substance or phenomenon with regard to several directions. In the field of materials science, for instance, a substance's mechanical, electrical, or thermal properties may be anisotropic, meaning that their values change according on the direction in which they are measured.

On the other hand, isotropy refers to the state in which a phenomenon, system, or property is uniform and displays the same traits in every direction. To put it another way, an isotropic substance or system exhibits symmetry along all orientations or axes. According to material science, materials that are isotropic share the same mechanical, electrical, and thermal characteristics in every direction. An isotropic material, for instance, would behave and have the same strength no matter how much force was applied to it.

Anisotropy, as opposed to isotropy, is the absence of symmetry or homogeneity with regard to various orientations in a substance, phenomena, or system. Thus, anisotropy denotes features that change or are directionally dependent, whereas isotropy denotes a condition of absolute homogeneity.

2.9 Anisotropy of WAAM sample

(Hassel & Carstensen, 2020) conducted a study on a deposited nickel alloy 617. The main objective of the study was to ascertain the mechanical characteristics of the as-welded state; to this end, tests for static strength, microhardness, and metallographic analyses were carried out. The anisotropic material behavior in relation to the build direction (BD) was tested. The direction-dependent strength characteristics of single-track welded structures

are illustrated with samples that were assessed at 0° , 45° , and 90° to the BD as shown in Figure 2.12.

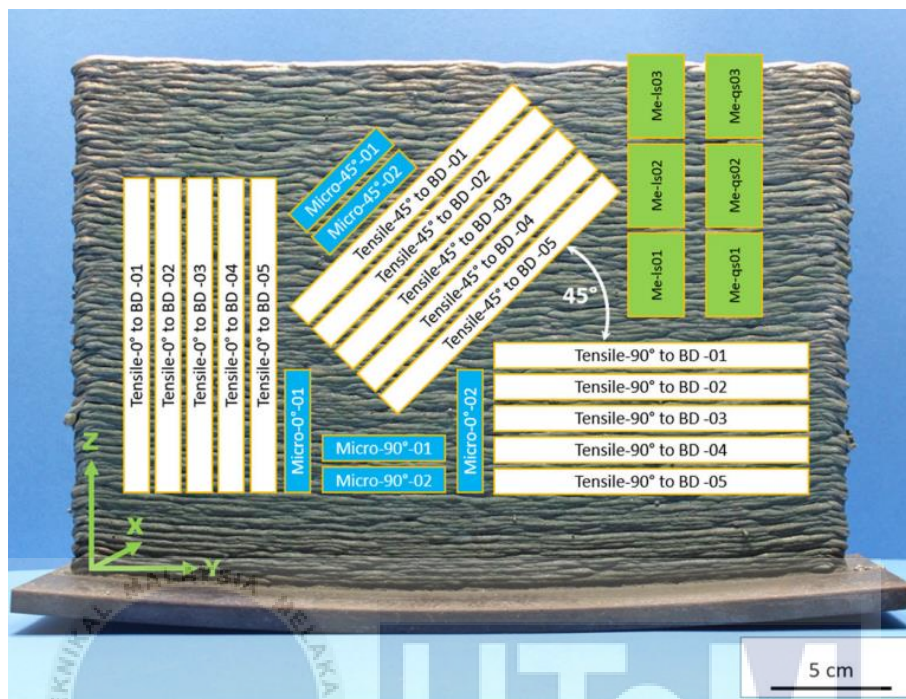


Figure 2.12 Cutting plan(Hassel & Carstensen, 2020)

The investigation revealed that the material's hardness and mechanical characteristics are not uniform in all directions. They are influenced by the direction known as BD. however it is difficult to draw firm conclusions because there is some overlap in the measured values.

Although the material loses flexibility, it gets stronger when oriented 45° toward BD. The mechanical characteristics are comparatively similar in the 90° to BD directions. There are two sliding systems operating at build direction 90° to BD, but only one is operating at build direction 45° to BD, indicating the existence of a dominant crystallographic direction.

(Sun et al., 2020) conduct a similar study which is anisotropy properties on WAAM produced sample but using a low-carbon high-strength steel which also produce a similar result. The longitudinal specimen exhibits mechanical properties that are not as strong as those of the transversal specimen, suggesting the presence of anisotropy. In the longitudinal

tension test, stress concentration and localized high strain are revealed by an analysis using the Digital Image Correlation (DIC) technique. It is believed that the high density of the inter-layer region which is regarded as a softened area and results in strain concentration is the cause of the longitudinal specimen's decreased mechanical performance.

2.10 Stainless Steel

The article (Jin et al., 2020) presents an overview of stainless-steel Wire Arc Additive Manufacturing (WAAM), highlighting its widespread use attributed to favorable mechanical properties and exceptional resistance to corrosion. The review covers a wide range of topics, including defects, mechanical characteristics, and microstructure related to various types of stainless steel and process variables. The conversation also includes residual stress and distortion in WAAM-manufactured components. Notably, particular procedures, material compositions, process parameters, shielding gas composition, post-heat treatments, microstructure, and defects can all have a major impact on the mechanical properties of WAAM stainless steels. In order to optimize the parameters of both WAAM and heat treatments and thereby regulate the microstructure, more research into the basic physical metallurgy mechanisms of the WAAM process and post-heat treatments is necessary to produce high-quality WAAM stainless steel parts. It is important to note that the mechanical properties and microstructure of WAAM samples frequently show significant anisotropy. On the other hand, the novel in-situ rolling + WAAM method works extremely well to mitigate residual stress and distortion while also reducing anisotropy (Jin et al., 2020).

In a study conducted by (Jin et al., 2020), WAAM is a cost-effective method for making large stainless steel parts. Recent studies have examined different aspects of WAAM for

stainless steels, including how the parts look, how their structure develops, how heat treatments affect them, and their mechanical properties.

A number of variables, including wire speed, scanning speed, welding current, cooling time, and interlayer temperature, affect how WAAM stainless steel parts look. To maximize these factors and raise the precision and caliber of WAAM parts, more investigation is required.

The balance between the austenite and ferrite phases, in particular, is dependent upon temperature variations during the manufacturing process on the structure of WAAM parts. We can accomplish the required structure by regulating the manufacturing temperature, employing double wires, or applying heat treatments. It's critical to comprehend how the final structure of WAAM stainless steel parts is influenced by the materials, manufacturing processes, and heat treatments.

2.11 Comparison of research gap

Both studies show that either direction will produce anisotropic behavior. Anisotropic materials may display differences in their performance, strength, or other attributes depending on the orientation in which they are applied. This variability can lead to irregularities in product quality and the structural integrity of components. Anisotropy in structural materials can give rise to weaknesses or susceptibilities in particular directions, which could potentially jeopardize the safety and dependability of structures and components. Although anisotropy is an inherent property in many materials and systems, it introduces challenges that must be overcome to ensure the products meet the expected performance standards.

2.12 Summary or research gap

In contrast to anisotropic characteristic, isotropic properties need to be achieved to solve the issue. Since their characteristics remain constant in all directions, isotropic materials are generally preferred. This consistency is very helpful in building structures and products that can be relied upon. Isotropy simplifies the prediction of material behavior, which facilitates the design of parts and structures that function consistently in a variety of orientations and environments. Since isotropy eliminates the need to take direction-dependent properties into account during the design and manufacturing processes, it frequently improves the efficient use of materials and resources in real-world engineering applications.

Addressing these research gaps would contribute to the further advancement and implementation of WAAM and machining in various industries. It would enable manufacturers to harness the full potential of these techniques, optimize their processes, and produce high-quality components with improved efficiency and performance.



3 CHAPTER 3

METHODOLOGY

3.1 Introduction

The methodology employed in this research aims to investigate the effects on different welding surface angle in terms of mechanical properties and microstructure on SS308LSI steel produced by wire and arc additive manufacturing.

3.2 Flow Chart

A visual representation of the sequential steps and logical progression of the research process is provided by the flowchart used in the technique. It accomplishes a number of significant tasks. The flowchart helps researchers efficiently organize and coordinate their operations. They can use it to visualize the entire research process, identify possible obstacles or areas that require further funding, and then allocate time and resources appropriately. This encourages effective project management and aids in achieving research goals within the allocated time period. The flowchart enables an efficient and organized presentation of the study technique. Readers can readily follow the study's step-by-step progression because it visually illustrates the logical flow of the activities as shown in Figure 3.1.

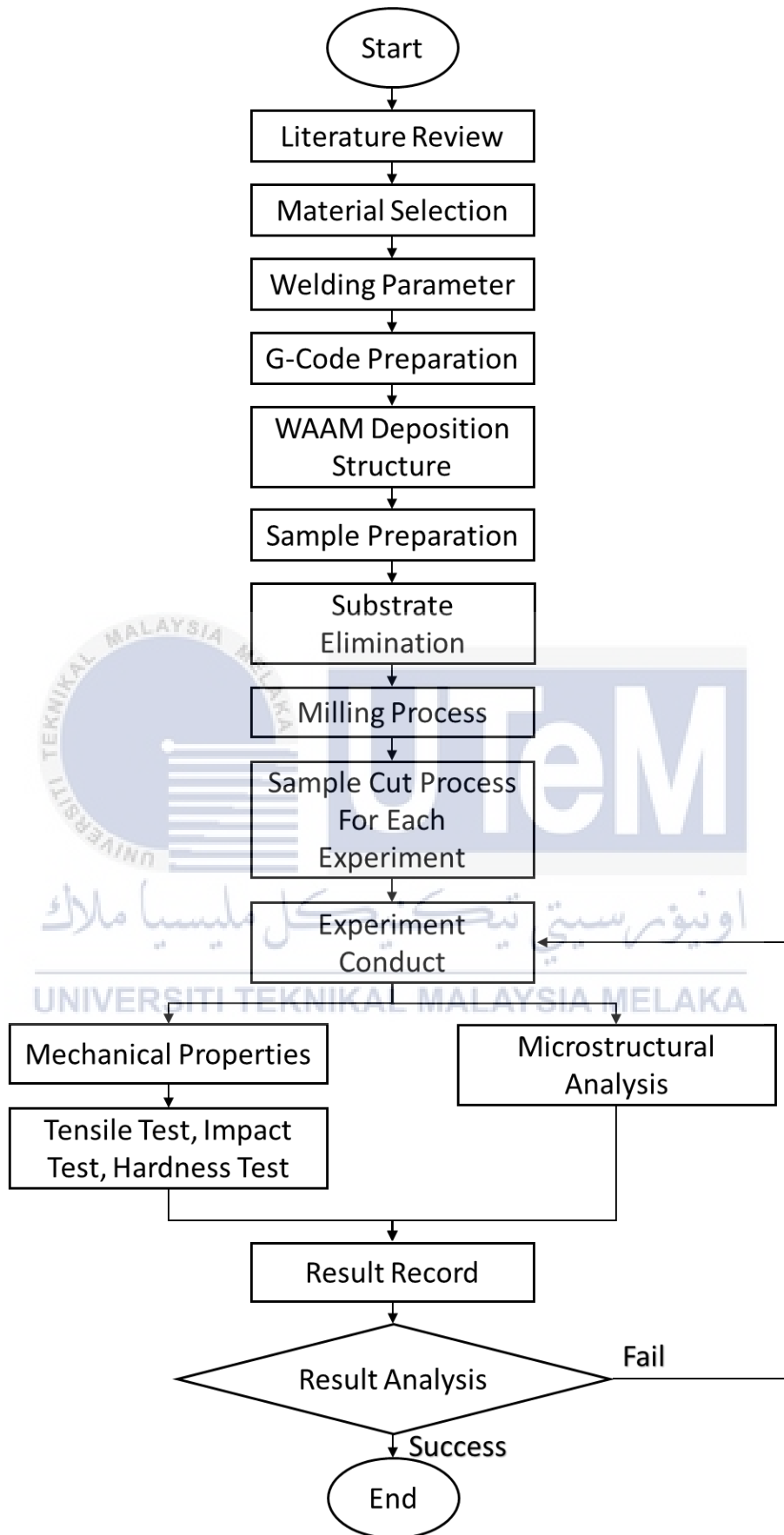


Figure 3.1 Flowchart

3.2.1 Stainless Steel 308LSi

Grade 308L stainless steel as shown in Figure 3.2 is a low carbon material highly suitable was chosen for its ideality for situations where there is a requirement for effective protection against atmospheric corrosion. It is a welding wire selected as a welding material that was deposited by the WAAM machine. 308LSi stainless steel chemical composition is shown in Table 3.1 and its mechanical properties are shown in Table 3.2 as provided by manufacturer.

Table 3.1 Deposited Chemical Composition % of 308LSi Stainless steel

C	Cr	Ni	Mn	Si	P	S
0.016	20.65	10.0	1.65	0.85	0.016	0.008

Table 3.2 308LSi Stainless Steel Mechanical Properties

Material	Ultimate Tensile Strength		Offset Yield Strength		Elongation (%)
	psi	MPA	psi	MPA	
308LSi	84100	580	58000	400	41



Figure 3.2SS308LSi Stainless Steel LSi

3.3 Machine Setup

Wire Arc Additive Manufacturing (WAAM) machine setup involves configuring various components to ensure precise control during the additive manufacturing process such as WAAM parameter, substrate, positioner and shielding gas. WAAM machine setup is a critical phase that requires careful calibration and configuration to achieve optimal results. The choice between gantry systems and robot manipulators, as well as the selection of deposition tools and material feed systems, depends on the specific requirements of the application. Regular maintenance and calibration are essential to ensure consistent and high-quality additive manufacturing.

3.3.1 Selection of WAAM Parameter

Three crucial welding process variables was carefully selected and kept an eye on for WAAM. These variables are wire feed rate, welding voltage, and welding current. The CMT power source machine has a manufacturer setting that will set all of the parameters to be proportional to each other when any parameter is set or chosen to ensure the best welding and deposition result. In this study, wire feed speed is the parameter chosen to be set and other parameter which is current and voltage will be set accordingly and automatically by the CMT power source due to manufacturer setting. The parameters that were used are 4m/min wire feed rate and the other parameter was set accordingly by the CMT power source as shown in

Table 3.3. Based on the parameter as followed, it produces a triangular wall as shown in Figure 3.3. Only four sample was produced due to time limitation and availability of the robot welding machine.

Table 3.3 ABB Robot Welding Parameter

Wire Feed Rate	Voltage	Current
----------------	---------	---------

(m/min)	(V)	(A)
4	12.4	140

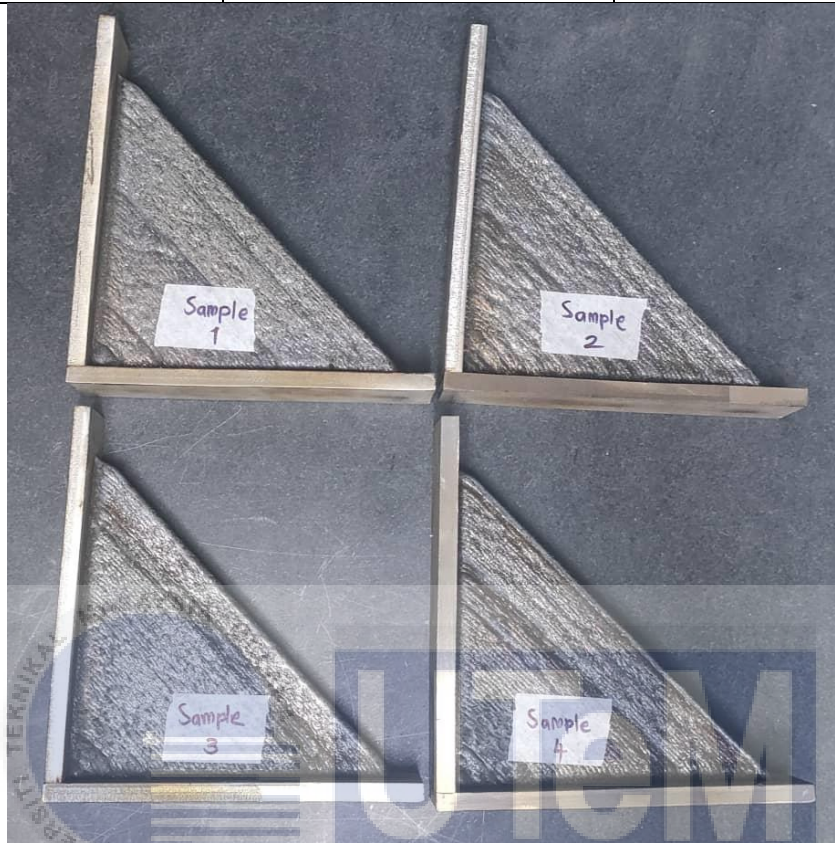


Figure 3.3 ABB robot welding produced wall

3.3.2 Jig for Substrate

The substrate needs were supported by a jig to hold it at 90° angle. A jig that were angled at 90° degree were built. Material that was used to build the jig is the same material that were used as the substrate which is 402 stainless steels. Two side of the 402 stainless steels went through a face milling process to get the most precise 90-degree angle. Both sides then welded to other 402 stainless steels plate to act as a jig surface to attach the substrate. The jig were clamped to the tilted work table and to the substrate which is the material that were used as a welding surface as shown in Figure 3.4.

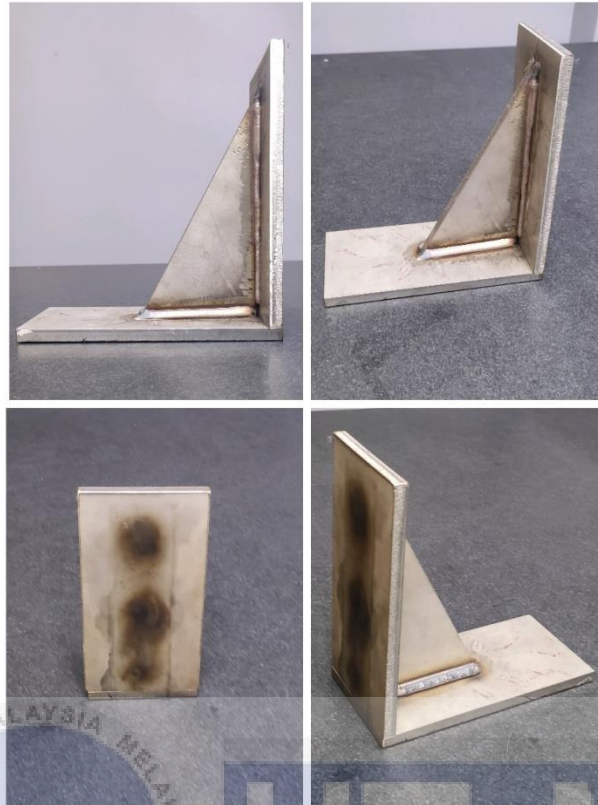


Figure 3.4 Support Jig

3.3.3 Positioner

Welding on a flat surface require no such change on the position of the work table. But to obtain the objective of welding on an angled surface, work table wa set to tilt at an angle of 45° as shown in Figure 3.5. the table was tilted to accomplish deposition on an angled surface. The other option is to build two 45° jig and placed on both side of substrate so the machine can proceed with deposition process without tilting the table. But to save time, 90° jig were used on only one side of the substrate while the other substrate was clamped on the table while the table tilt. Thus, produce a 45° on each substrate as shown in Figure 3.6.

The tilted table was achieved through a 3DP software which is the software for the ABB robot welding which will be explain later in this chapter.

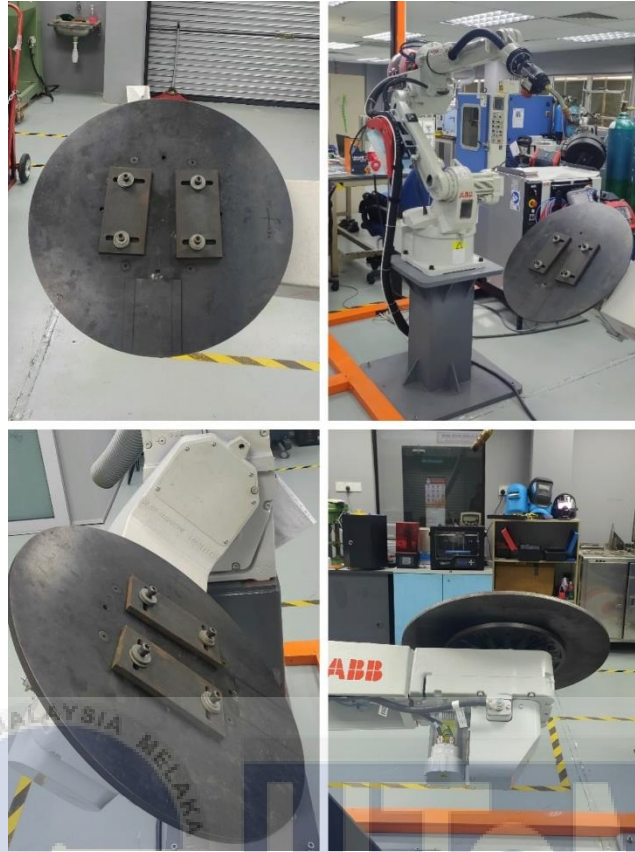


Figure 3.5 Tilted work table



Figure 3.6 Tilted Work Table with substrate clamped

3.3.4 Shielding Gas

Shielding gas as shown in Figure 3.7 are used during deposition process to serve its purpose which is to safeguard the molten weld pool from being exposed to oxygen, nitrogen, and hydrogen present in the surrounding air. When these elements react with the weld pool, it can lead to various issues like the formation of holes (porosity) within the weld bead and excessive spatter. An Argon-Oxygen 98% to 2% are used as a shielding gas because a 2%

oxygen blend is an ideal choice for spray transferring stainless steel. It is used for spray arc welding of carbon and low-alloy steels. It creates a greater wetting action than the 1% oxygen mixture. The vaporized gas is sprayed with a flowrate of 25 l/min.



Figure 3.7 Shielding gas

3.4 Software

To obtain the desired outcome of depositing on a 45° welding surface, four software are used to obtain the G-code. G-code functions as a programming language applied in computer-aided manufacturing (CAM) and computer numerical control (CNC) machines, serving as a collection of directives that guide CNC machines in the execution of movements, control operations, and the operation of machinery for the production of parts

and components. ABB robot welding as the CNC machine also use G-codes to translate the movement during deposition process.

3.4.1 SolidWorks

The initial steps before obtaining the G-code are to have the drawing of desired shape of the later deposited wall. Thus, SolidWorks come in play. SolidWorks is a widely used computer-aided design (CAD) software application developed by Dassault Systèmes. It is known for its powerful and versatile capabilities in 3D modeling and design. The drawing is an easy step as the desired deposited wall are a simple triangle shape. The important steps are to save the file as an STL file.

STL file are is a frequently employed file format in the realms of 3D modeling and 3D printing. This format depicts the structure of a three-dimensional object by utilizing a set of interlinked triangles or facets, which in turn delineate the object's form and surface characteristics.

3.4.2 Cura

Cura is a software application used in the field of 3D printing. It is primarily known as a slicing software, which means it takes 3D models created in computer-aided design (CAD) software and converts them into a series of instructions (G-code) that 3D printers can understand and execute.

Cura are used to import 3D models in various file formats, which in this case, the STL file and prepare them for 3D printing. This includes tasks such as scaling, positioning, and orientation adjustments.

One of Cura's primary functions is slicing 3D models into thin horizontal layers. It generates the G-code instructions required for the 3D printer to build the object layer by layer. Users

can configure various slicing parameters, such as layer height, infill density, and print speed, to customize the printing process.

Cura also provides a visual representation of how the 3D print will progress layer by layer. This feature allow user to see the deposition process layer by layer. Cura supports a wide range of 3D printers and allows users to select their specific printer model to optimize settings for that machine including ABB robot welding.

3.4.3 Repetier

G-code generated by Cura were imported to Repetier. Repetier allow user to better see the tool path of the deposition process by each layer. This include where the nozzle will deposit the welding material and where not to. The crucial function of this software is to modify the G-code.

G-code provided by Cura will translate to physical movement of the nozzle in a raster tool path. Repetier allow user to modify the G-code to translate from raster tool path to zig-zag formation tool path while overseeing the displayed tool path movement on the software. This allows user to observe if any error occurring while modifying the G-code. Zig-zag tool path will shorten the time of deposition as the nozzle will take less time to move to the next layer without returning to the previous side of the wall.

3.4.4 3DP

3DP is a designed software purposely for ABB robot welding to translate the movement of the robot and also the work station where the welding plate are clamped. The crucial function of 3DP is to set the initial position of the nozzle on where to start the process with visual representation of the ABB robot welding machine displayed on the software. This step is crucial as to obtain the best desired outcome of deposited wall. Without 3DP software, user

have to manually set the initial point of deposition using the teach pendant which is a multistep procedure and can take a long time to do so.

The G-code and the initial position setup is transferred to the ABB robot welding through a LAN cable connected to the ABB robot welding.

3.5 Sample Preparation

Sample produced by WAAM has a certain characteristic that need to be addressed before it can undergo the test and analysis process. WAAM use a welding concept thus the produced sample has welding characteristic which is the surface waviness. Other than that, WAAM use a 304L stainless steel as a substrate where the deposition process occurs. Thus, the substrate needs to be removed from the sample produced.

3.6 Horizontal Band sawing Machine PR-10V.

Cutting is the act of dividing a material into multiple segments, constituting a subtractive manufacturing process wherein material is extracted from the workpiece to achieve the intended shape and features. Thus, the substrate was removed by using a horizontal band saw machine as shown in Figure 3.8.



Figure 3.8 Horizontal Band sawing Machine PR-10V

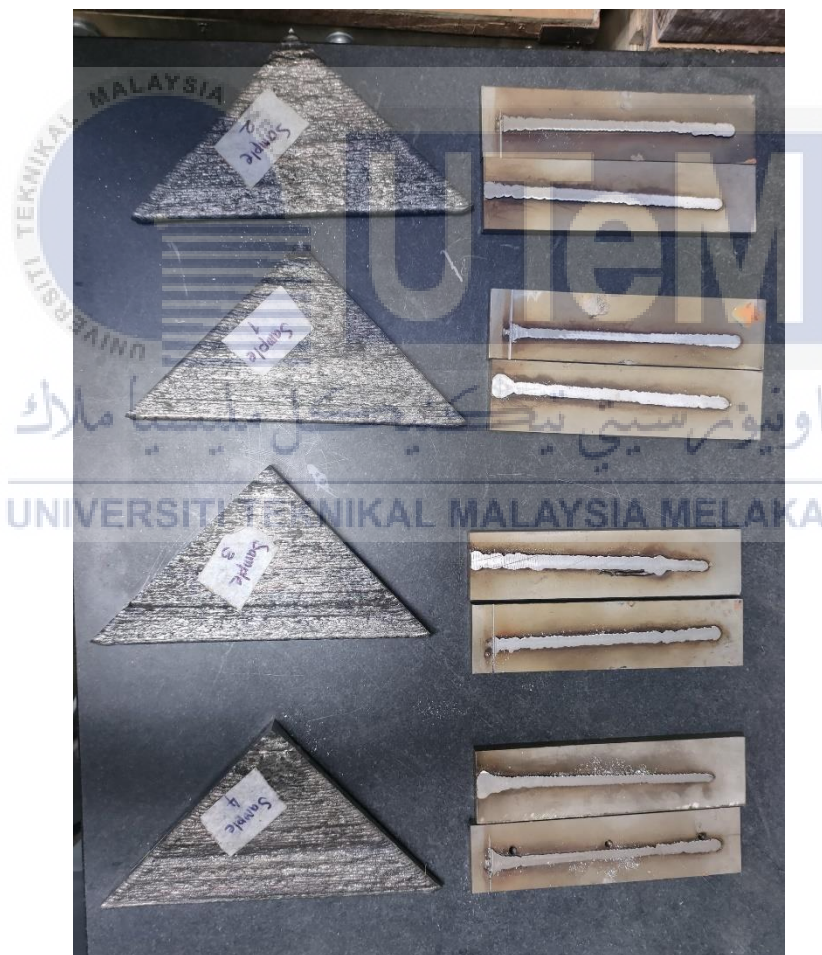


Figure 3.9 Sample after cutting process

3.6.1 Electrical Discharge Machine (EDM) Wire Cut

Wire-cut EDM is a commonly employed technique for cutting plates up to a thickness of 300 millimeters. It is also utilized in the production of challenging-to-make punches, tools, and dies from hard metals, which are difficult to manufacture using traditional methods. In this process, the wire was held in place by upper and lower diamond guides, while the entire setup is centered within a water nozzle head. The wire then continuously unwound from the spool without stopping. Water served as the dielectric fluid in the wire-cutting process, and its resistivity and other electrical properties are controlled using filters and PID-controlled de-ionizer units. The water effectively carries away the debris resulting from the cutting process.

The EDM wire cutter that are used are Sodick VZ300L made by the Germans as shown in Figure 3.10. The wire cutter is an essential and crucial machine to be used as it offers precision in cutting a material which in this study, the 308LSi stainless steel. The machine uses 0.25mm diameter brass EDM wire as shown in Figure 3.11. It was chosen as the wire have high tensile strength and low vaporization point which made it a great electrode material. Its performance and precision offer a great option to cut complex shape for tensile test and Charpy impact test specimen according to ASTM E8 for tensile test and ASTM E23 for charpy impact test as shown in Figure 3.13 and Figure 3.14. All 4 sample undergo the same process for all tensile and impact test specimen to be acquired. Table 3.4 shows which side on each sample



Figure 3.10 Sodick VZ300L EDM wire-cut machine.



Figure 3.11 0.25mm diameter EDM wire

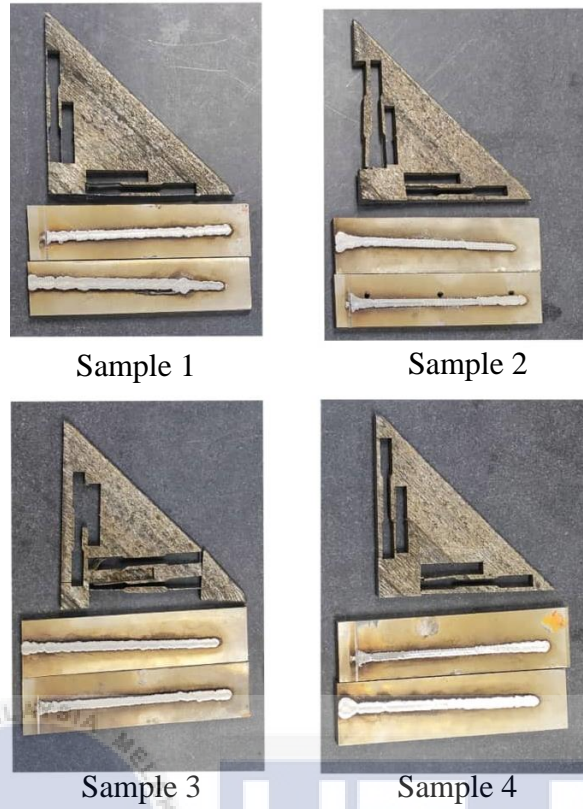
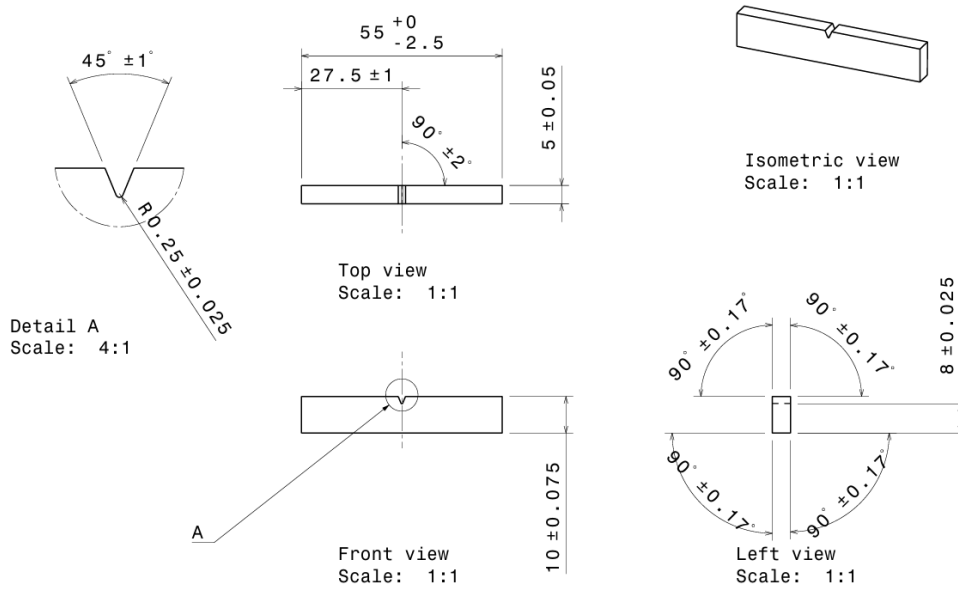


Figure 3.12 Sample after wirecut process



Figure 3.13 Tensile test specimen dimension according to ASTM E8



Unit: Millimeter (mm)

Charpy specimen; thickness 5.0 mm

Figure 3.14 Charpy impact test specimen according to ASTM E23

Table 3.4 Side for each sample

<p>Side A</p>	
<p>Side B</p>	

3.6.2 Milling Machine

The milling process involves the removal of material from a workpiece using rotary cutters, which execute the cutting action. This was achieved by adjusting the direction on one or more axes, as well as the speed and pressure of the cutter head. In addition to grinding and turning materials, milling machines are also referred to as multitasking machines (MTMs). The WAAM fabricated sample has a waviness surface characteristic while the specimens for the tensile test and Charpy impact test require a flat surface thus the milling machine come into play. It was included to remove the waviness surface characteristic of the sample fabricated by WAAM. Thus, a milling machine, equipped with a cutter aid in the removal of material from the surface of the workpiece were used to solve the waviness surface of each specimen. Once the material has cooled, it is extracted from the milling machine. In this experiment, an FM-16VS model manufactured in Taiwan in 2012 was used. Figure 3.15 depicts the milling machine.



Figure 3.15 FM-16VS Milling Machine

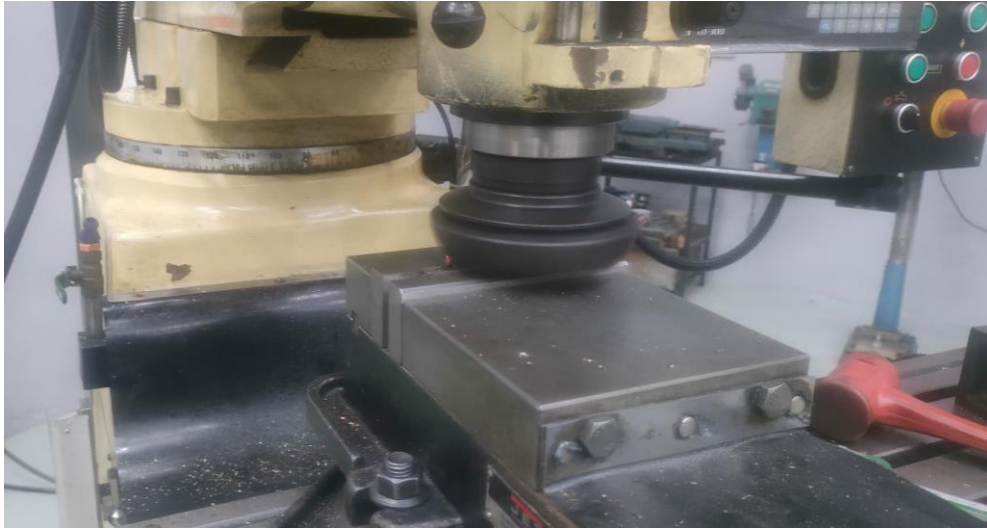


Figure 3.16 Milling process

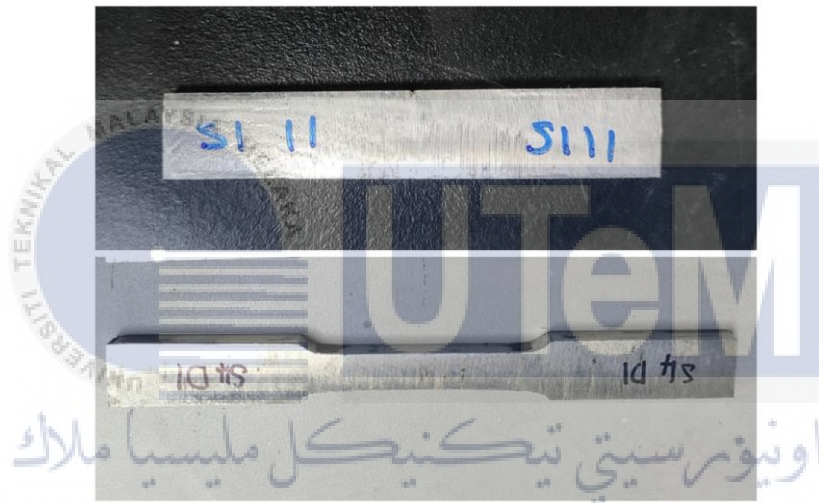


Figure 3.17 Tensile and impact specimen after milling

3.7 Mechanical Properties

The way a material responds to external forces or loads is determined by its mechanical characteristics. These attributes play a vital role in the design and engineering of components across various industries as they offer valuable insights into the material's behavior under different conditions. In order for manufactured products to exhibit reliability, optimal performance, and structural soundness, a thorough comprehension of a material's mechanical properties is absolutely essential.

3.7.1 Tensile Test

The utilization of a tensile testing apparatus in the context of Wire Arc Additive Manufacturing (WAAM) serves the primary function of evaluating and analyzing the mechanical attributes of structures or components created through WAAM. This evaluation specifically focuses on characteristics like tensile strength, yield strength, and elongation. Tensile testing represents a standardized technique that involves applying axial tension to a test specimen until it fractures. Figure 3.18 show the tensile test machine used for this purpose and Figure 3.19 shows tensile specimen before and after the tensile test for each sample. The parameter that was used is 5mm/min for the crosshead speed.



Figure 3.18 Floor Mounted Material Testing System. Instron Model 5585 Capacity 200KN.

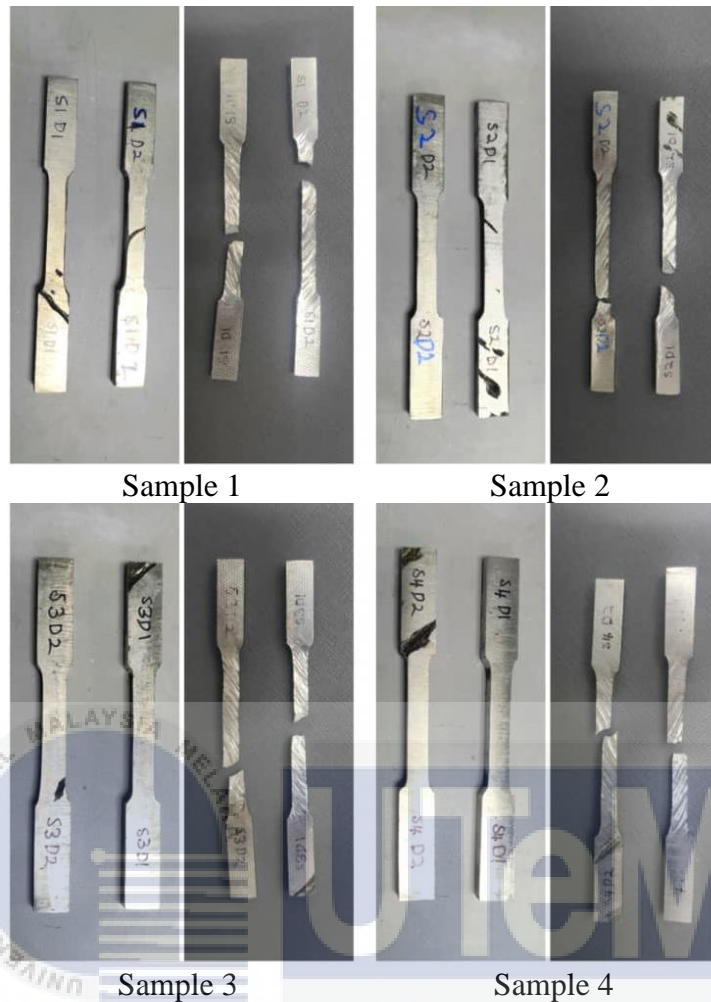


Figure 3.19 Tensile specimen before and after tensile test

3.7.2 Charpy Impact Test

The objective of performing Charpy impact assessments within the realm of Wire Arc Additive Manufacturing (WAAM) is to evaluate the impact durability and resilience of structures or components fabricated through WAAM processes. Charpy impact testing represents a standardized approach employed to quantify the energy absorbed by a material when it fractures due to a swinging pendulum impact. In WAAM, where the additive manufacturing procedure entails the incremental deposition of material layer by layer, it becomes imperative to scrutinize mechanical attributes, particularly those related to impact resistance. Figure 3.20 and Figure 3.21 illustrates the Charpy impact test machine and Charpy impact specimen before and after the test. The parameter of the test is shown in Table 3.5.



Figure 3.20 Charpy Impact Test Machine



Figure 3.21 Charpy impact specimen before and after impact test

Table 3.5 Charpy impact test parameters

Impact energy (J)	Impact speed (m/s)	Pre-rising angle of pendulum (°)	Thickness of impact blade (mm)	Power supply	Net weight (kg)
250	5.24	150	16	380V and 50Hz	550

3.8 Hardness Test

Performing hardness tests in Wire Arc Additive Manufacturing (WAAM) is crucial for evaluating the mechanical properties of the produced components and verifying their compliance with specified requirements. The hardness test aids in gauging the material's ability to withstand indentation or scratching, offering valuable insights into its strength, durability, and appropriateness for particular applications. Figure 3.22 shows the Vickers Hardness Tester. Shimadzu HMV-G31 and the parameters for the hardness testing are shown in Table 3.6. Hardness sample were done in the side A from sample 3.



Figure 3.22 Vickers Hardness Tester. Shimadzu HMV-G31.

Table 3.6 Micro-Vickers hardness testing parameter

Indenter	Diamond
Load	19.61 N
Indented time	10 s

3.9 Microstructural Analysis

The microstructure of a part manufactured through Wire Arc Additive Manufacturing (WAAM) is shaped by multiple factors, encompassing welding parameters such as arc current, voltage, travel speed, and wire feed rate, alongside material properties and composition. Grasping and managing the microstructure are pivotal as it directly impacts the mechanical properties and overall performance of the final fabricated part. In this study, the same parameter was used and the hardness result were acquired from the same sample but different region which is the top, middle and bottom region.

3.9.1 Hot mounting

In metallography, hot mounting is a sample preparation method frequently used to get specimens ready for microscopic examination. Using this technique, a metal sample is heated to high pressures and immersed in a thermoplastic substance. The objective is to produce a mounting to mount the sample for grinding and polishing process. The Mounting press machine Ecorpes 100 as shown in Figure 3.23 and its parameter in Table 3.7.



Figure 3.23 Mounting press machine Ecorpes 100

Table 3.7 Mounting press machine parameter

Heating temp (°C)	Pressure (atm)	Heating time (minute)	Mould size (mm)	Cool temperature (°C)	Type of powder
180	200	4	25	35	Phenolic powder

3.9.2 Grinder and polishing machine

Polishing and grinding are essential steps in the metallographic sample preparation process, particularly when examining microstructures using microscopy. These processes help achieve a smooth and flat surface, revealing the internal structure of the material under examination. The sample with the mounting was mount on the grinder and polishing machine as shown in Figure 3.24. The sandpaper was placed on the plat that rotate 200rpm clockwise while the mounter pressing the sample toward the rotating plate was rotating 90 rpm anti-

clockwise to optimized grinding process time with water act as a cooling, lubrication, debris removal, and corrosion prevention agent as shown in.

The process was repeated with different sandpaper grit from 200, 320, 600, 800, and 1000 grit. The process then proceeded with polishing process with ultra-fine abrasive polishing cloth twice. The polishing cloth have diamond particles embedded in the polishing cloth allowing them to effectively abrade and polish the sample. The first polishing cloth are 3μ and the second polishing cloth are 1μ . The term micron(μ) is a unit of measurement equal to one millionth of a meter. In the context of polishing cloths, the micron size corresponds to the diameter of the abrasive particles. All this process is to get a smooth surface of the sample as shown in before proceeding to microstructure analysis.

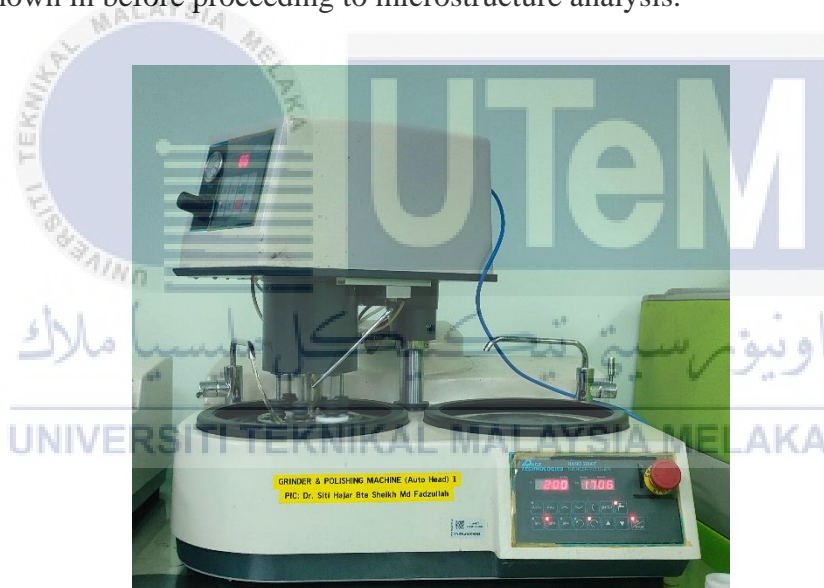


Figure 3.24 Grinding and polishing machine



Figure 3.25 Grinding and polishing process

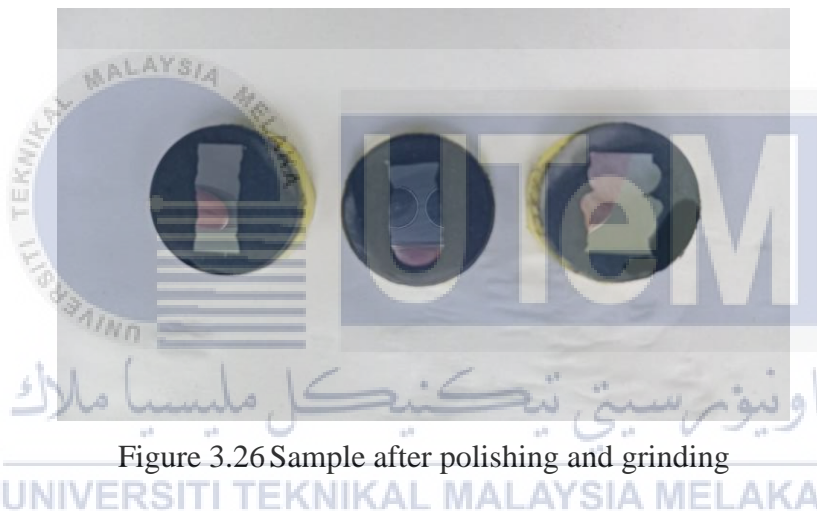


Figure 3.26 Sample after polishing and grinding

3.9.3 Optical Microscope

The utilization of an optical microscope within Wire Arc Additive Manufacturing (WAAM) serves the purpose of inspecting and scrutinizing the microstructure and surface attributes of structures or components constructed through WAAM at microscopic scale. Figure 3.27 displays the Nikon Eclipse Lv100 Microscope Machine used in this process.

One crucial step before microstructure analysis is the polished sample was etched into an etching solution specifically for stainless steel as shown in Figure 3.28 to burn to microstructure of the sample so the microstructure can be easily identified under the microscope. Figure 3.29 shown microstructure sample after etching.

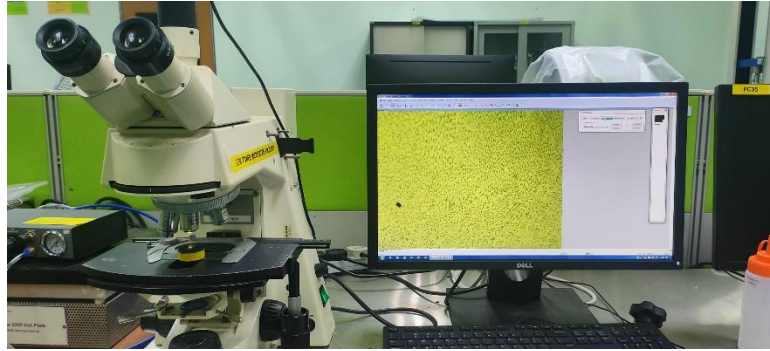


Figure 3.27 Nikon Eclipse Lv100 Microscope Machine.

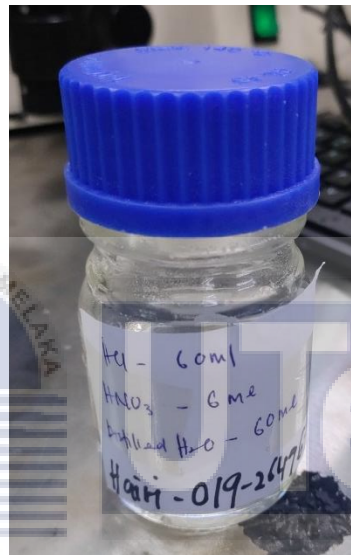


Figure 3.28 etching solution for stainless steel



Figure 3.29 Microstructure sample after etching

3.10 Summary

This chapter describes the materials, equipment, experimental setup and testing procedures of this research. The methods in developing the WAAM structure and study the different effect of welding surface angle are clearly explained. The characterization

procedure and analysis for the mechanical properties and microstructure in terms of tensile test, impact test and microstructure analysis are described in this chapter. Finally, the optimized parameter on the WAAM process will be determined to produce the best quality of the WAAM structure.



4 CHAPTER 4

RESULTS AND DISCUSSION

4.1 Introduction

This chapter presents and discusses the result of whether different direction of specimen cut from the sample will produce a similar result in other words, whether anisotropy was achieved. This chapter analyses the study of tensile test, charpy impact test, hardness test and microstructure analysis. It is been highlighted that this chapter covers the study of material strength of the WAAM structure which will be resulted into specimen according to ASTM E8 for tensile test and ASTM E23 for charpy impact test.

4.2 Tensile Test

The tensile test, a method of destructive testing, offers insights into the tensile strength, yield strength, and ductility of metallic materials by measuring the extent of stretch or elongation before reaching the breaking point. A crucial parameter in assessing a material's mechanical performance is its ultimate tensile strength, also referred to as tensile strength, representing its ability to withstand tension-induced breaking.

Tensile specimens, shaped like a dog bone and measuring 100mm x 10mm x 6mm, are precisely crafted using an EDM wire cut machine. The machine ensures accurate dimensions and produces a superior cut trace or surface, with a cutting diameter of 0.25mm.

In the field of mechanics, a material demonstrates strength if it can withstand applied force or stress without failing or undergoing plastic deformation. The material's behavior is illuminated through the creation of a stress-strain curve, allowing the identification of critical points such as the fracture point, yield point, and necking. The yield point marks the transition from elastic behavior to the initiation of plastic deformation, while the necking point indicates the point at which the material ultimately fails.

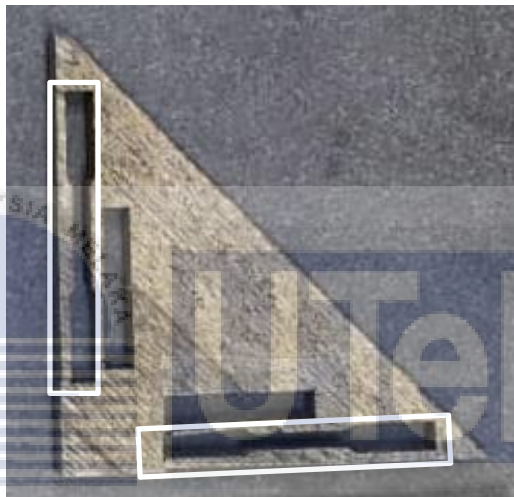


Figure 4.1 Tensile Test Specimen

4.2.1 Result of Tensile Test Specimen

The objective of the tensile test result was not focus on which side have a better mechanical property but rather whether both directions achieved isotropy properties. Figure 4.2, Figure 4.3, Figure 4.4, Figure 4.5 and Table 4.1 shows the result of the tensile test.

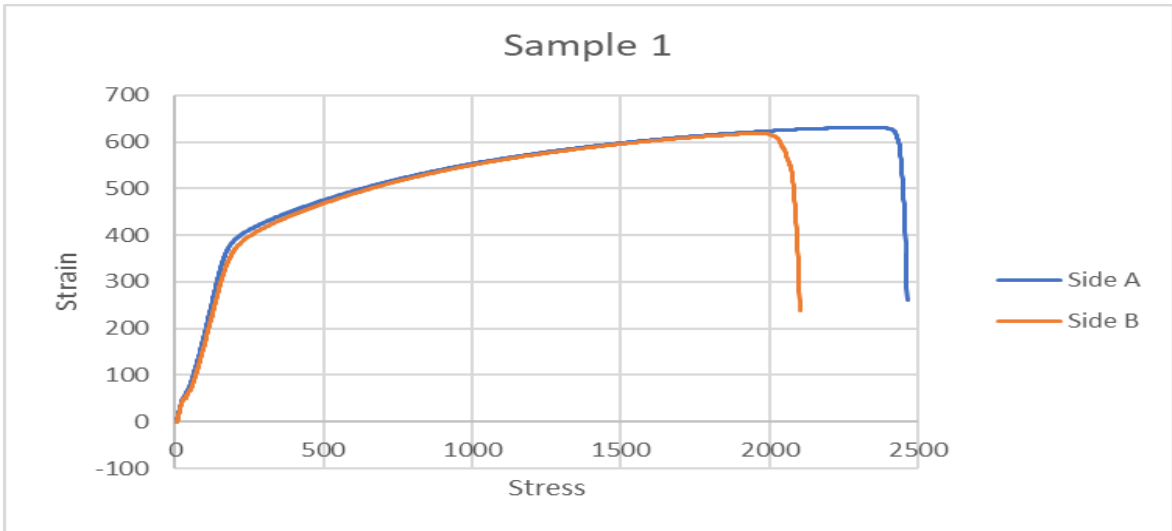


Figure 4.2 Sample 1 tensile test result

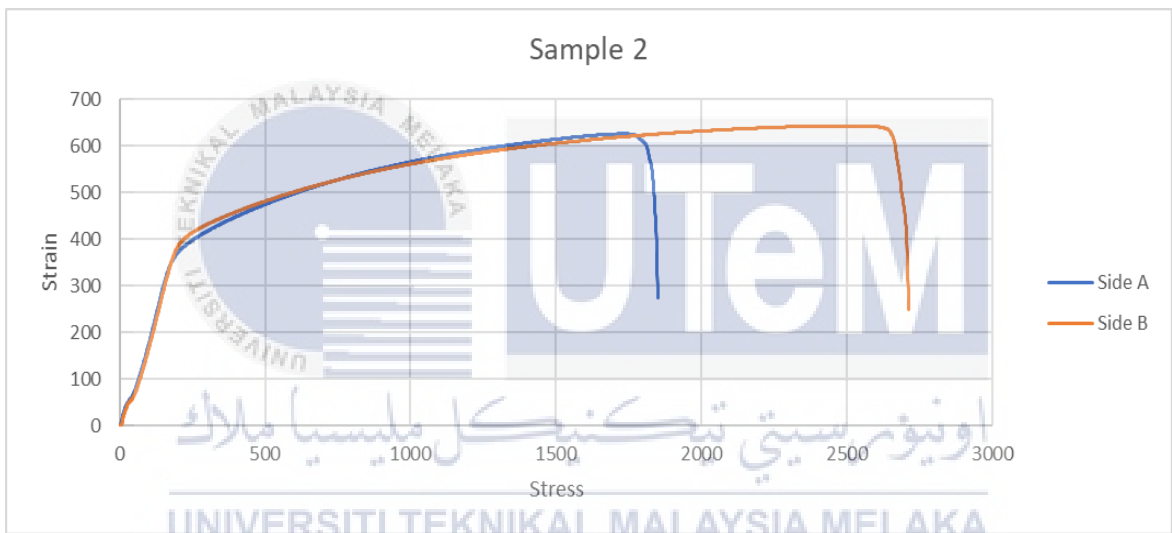


Figure 4.3 Sample 2 tensile test result

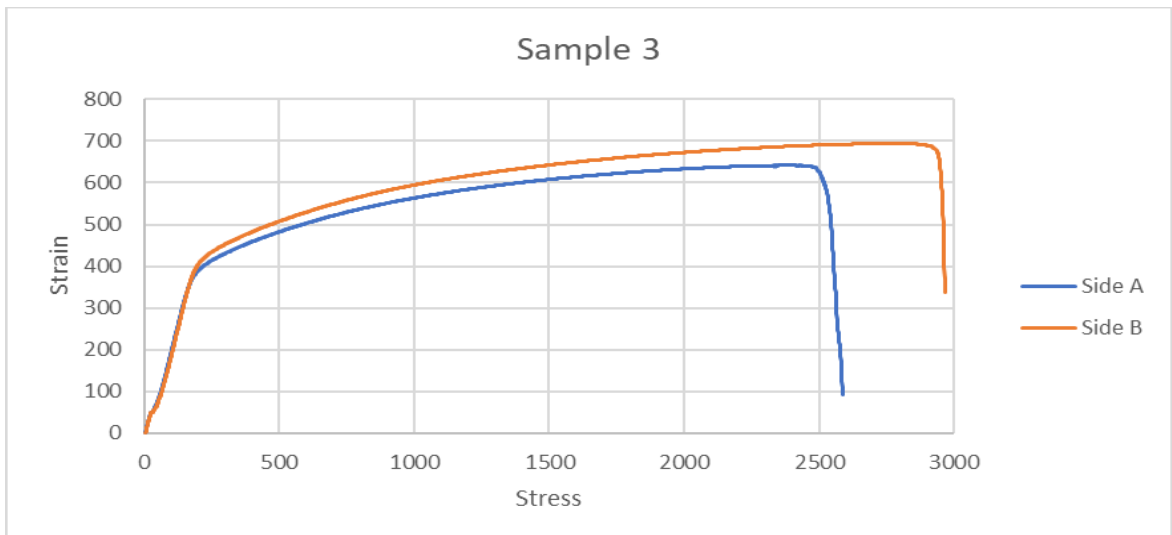


Figure 4.4 Sample 3 tensile test result

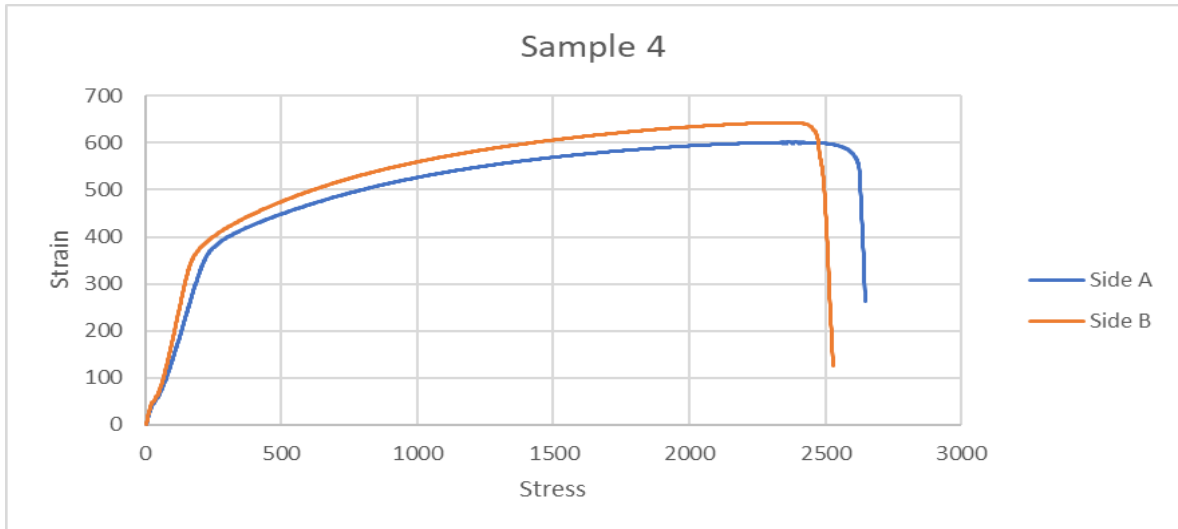


Figure 4.5 Sample 4 tensile test result

Table 4.1 Tensile test result

Sample	Specimen	Young's Modulus (MPa)	Maximum Load (kN)	Tensile stress at Maximum Load (MPa)	Tensile strain (Extension) at Maximum Load (mm/mm)
1	A	11339.551	22.721	631.137	0.484
	B	10976.599	22.276	618.773	0.405
2	A	10125.856	22.525	625.702	0.362
	B	9605.012	23.119	642.191	0.518
3	A	11637.512	23.101	641.708	0.497
	B	11062.643	24.995	694.317	0.580
4	A	8493.885	21.647	601.292	0.492
	B	10170.351	23.156	643.211	0.492

Based on the table, the specimen did fulfil its expected result as a 308 Lsi stainless steel. But the focus were more on to achieve anisotropy behaviour for all specimen on both side for each sample. To put into a conclusion, the difference of each side for each sample's mechanical properties and average difference of each mechanical properties is shown in Table 4.2 and Table 4.3.

Table 4.2 Both side difference for each mechanical properties

Sample	Young's Modulus (MPa)	Maximum Load (kN)	Tensile stress at Maximum Load (MPa)	Tensile strain (Extension) at Maximum Load (mm/mm)
1	362.952	0.445	12.364	0.079
2	520.844	0.594	16.489	0.156
3	574.869	1.894	52.609	0.083
4	1676.466	1.509	41.919	0

Table 4.3 Average difference for all mechanical properties

Young's Modulus (MPa)	Maximum Load (kN)	Tensile stress at Maximum Load (MPa)	Tensile strain (Extension) at Maximum Load (mm/mm)
783.783	1.111	30.845	0.08

Compared to other studies, the result for both sides still produces a different value for each side. As shown in Table 4.3, the maximum load total average at 1.111kN. The tensile stress at maximum load total average at 30.845MPa and tensile strain at maximum load total average at 0.08. Can be concluded that all data shows only small different between both sides compared to other studies. Thus, can be said that isotropy was achieved but not quite perfect enough.

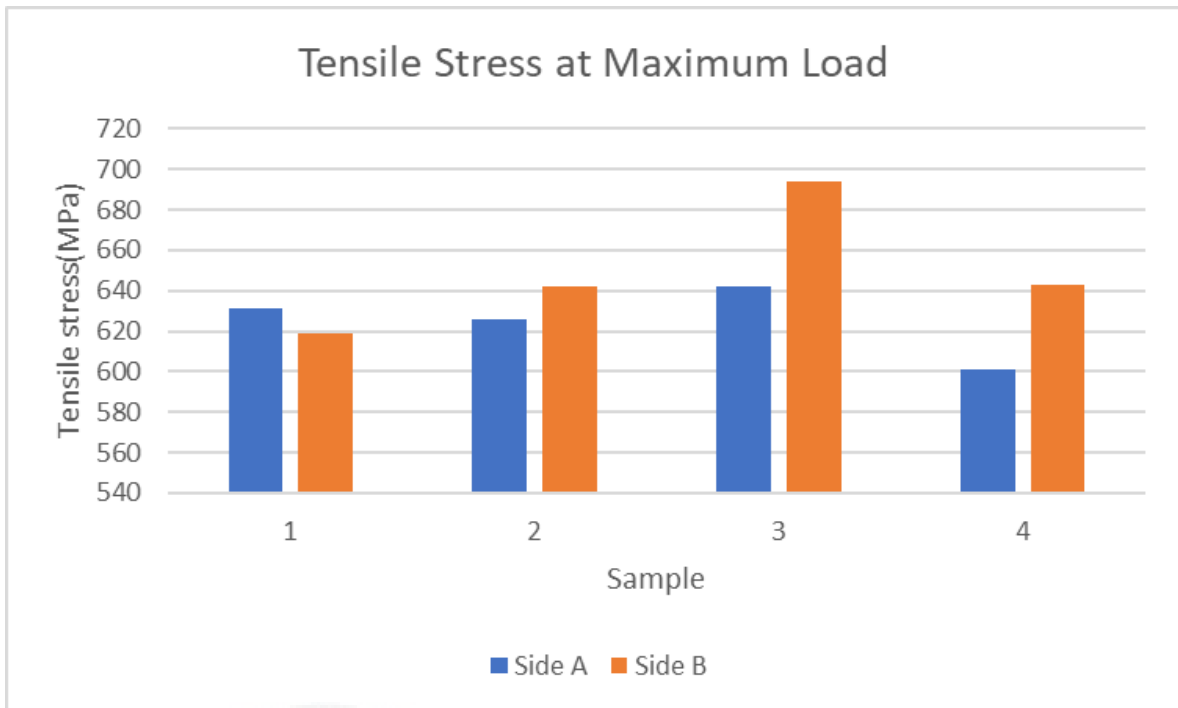


Figure 4.6 Tensile stress at maximum load

Based on Figure 4.6, side B from all sample produce a better tensile stress at maximum load except for sample 1. Thus can be conclude that side B is better compared to side A in terms of tensile stress at maximum load. The main aspects of the manufacturing process are the source of anisotropy in Wire and Arc Additive Manufacturing (WAAM). Material anisotropy is produced when weld material is deposited in layers during WAAM and solidifies under different circumstances (Hadjipantelis et al., 2022). Both side mechanical properties may vary due to the deposition direction with zig-zag toolpath that continuously heat the metal during deposition on both side. Machining process may also be a factor of this result. Work hardening is a consequence of some machining techniques, such as cold working. This could make the material stronger and harder, but it might also make it less ductile (Hadjipantelis et al., 2022). Thus explain those anisotropic behaviour on both side.

4.3 Charpy Impact Test

All specimens cut from each sample underwent the Charpy impact test with the primary objective of calculating the average data value. Each specimen measured 55x10x5 mm. The table provides a detailed record and presentation of the results observed on both the analogue scale and digital display.

The material's impact toughness is assessed through the impact test, which measures its tenacity and ability to withstand sudden loads while absorbing energy. The determination of toughness takes into consideration the ductility and strength of the material under examination. The Charpy test is conducted using a Charpy impact tester, Model JBW-500 Computer Pendulum Impact Testing Machine, in accordance with ISO 148-2 and ASTM E23.

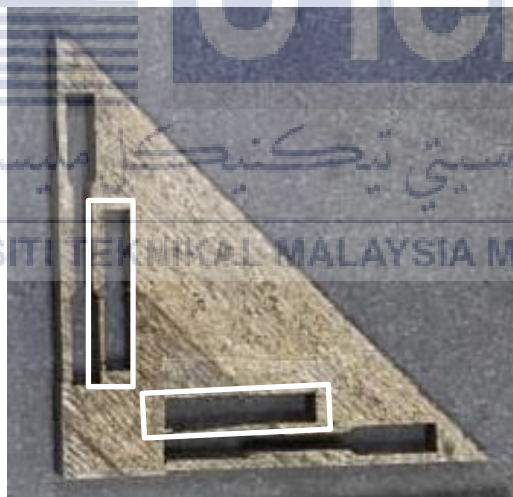


Figure 4.7 Charpy impact test specimen

4.3.1 Result of Charpy Impact Test Specimen

The result for charpy impact test is as shown in Table 4.4.

Table 4.4 Data for Charpy Impact Test Energy Absorbed

	Energy absorbed (J)	
	Side A	Side B
Sample 1	75.62	72.07
Sample 2	70.31	79.88
Sample 3	79.88	64.21
Sample 4	71.85	72.51
Average	74.42	72.17
Difference	5.618	

The result that were focused on charpy impact test is the energy absorbed. Table 4.4 shows that sample 1 and sample 4 shows quite significant isotropy result where it produce quite small difference on both sides with difference of 2.55J of energy absorbed on sample 1 and 0.66J of energy absorbed. In other hand, sample 2 and sample 3 shows quite big difference of both sides value of energy absorbed. Sample 2 produces difference of 9.57J and sample 3 produces differences of 15.67J of energy absorbed. Figure 4.8 displays the average value of energy absorbed on both sides for each sample in a bar graph. Figure 4.8 shows the impact specimen before and after the charpy impact test.

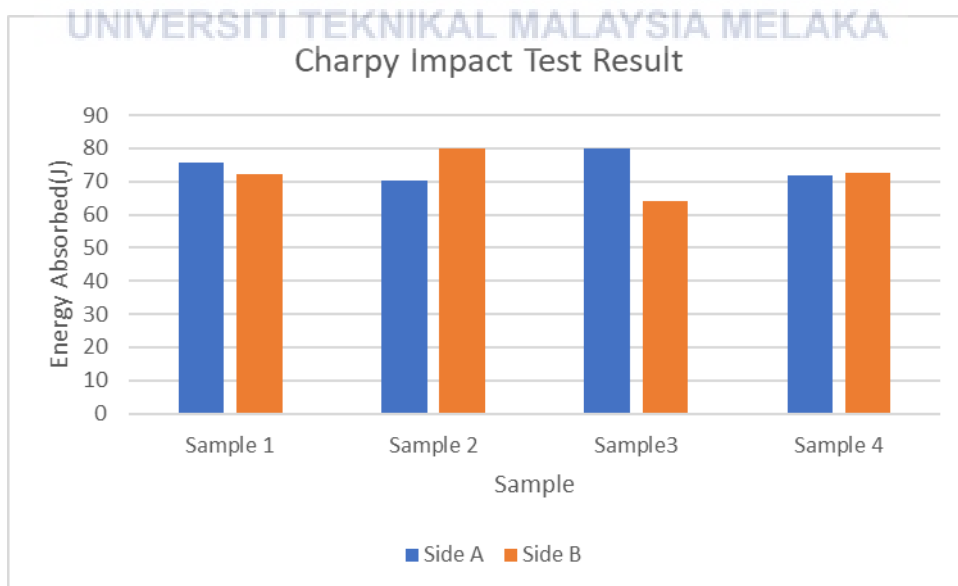


Figure 4.8 Charpy Impact Test result graph

Based on Figure 4.8 and Table 4.4, averagely, side A produce a better result in terms of energy absorbed compared to side B. The primary components of the Wire and Arc Additive Manufacturing (WAAM) process are the sources of anisotropy. When weld material is deposited in layers during WAAM and solidifies under various conditions, material anisotropy is created (Hadjipantelis et al., 2022). Because of the zigzag toolpath used for deposition, which continuously heats the metal during the process, the mechanical properties of both sides may differ. This outcome might also be influenced by the machining process. Some machining methods, like cold working, can lead to work hardening. This might increase the material's strength and hardness while decreasing its ductility (Hadjipantelis et al., 2022). Consequently, explain both sides' anisotropic behavior.

4.4 Microhardness Test

The Micro-Vickers hardness test reveals how hardness properties of different region on the sample were varies on each sample with top region with the lowest reading and bottom region with the highest reading. (Anand et al., 2023) in his study find that the middle zone of the manufactured slab appears comparatively softer than the top and bottom zones because of the significant impact of heat accumulation. Figure 4.9 and Table 4.5 shows result of Micro-Vickers hardness test.

Table 4.5 Sample 3 Micro-Vickers Hardness result

Region	No. of test	Micro-Vickers Hardness (HV)
Top	1	206.228
	2	217.193
	3	212.214
	4	208.592
	5	222.348
	Average	213.315
Middle	1	196.073
	2	190.753
	3	197.164
	4	184.649
	5	188.685
	Average	191.4648
Bottom	1	201.62
	2	196.073
	3	185.646
	4	209.789
	5	212.214
	Average	201.0684

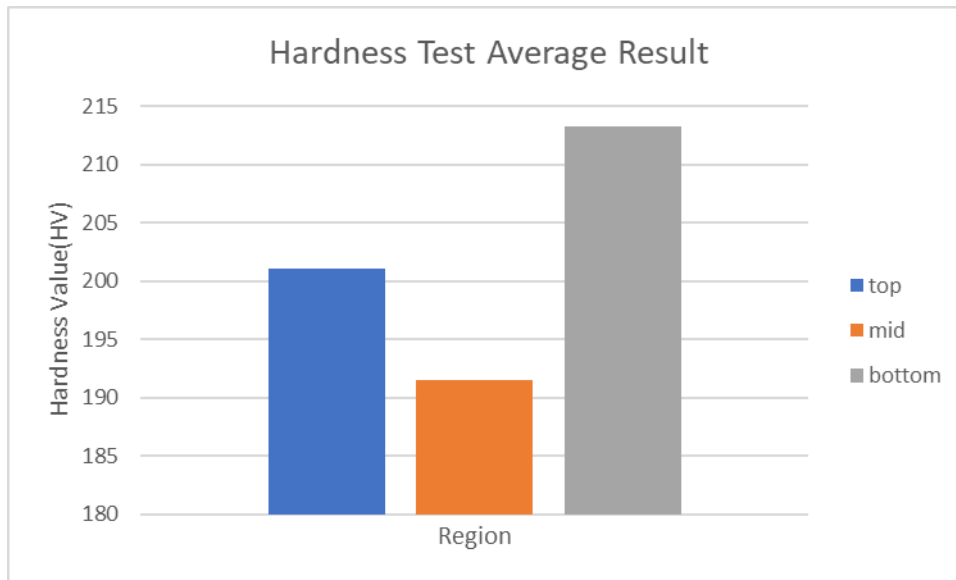


Figure 4.9 Micro-Vickers Hardness value graph

Figure 4.9 and Table 4.5 show a result for hardness test based on sample 3 on three different region which is top bottom and middle region for the Micro-Vickers hardness test. The results provide valuable information about surface hardness. The specific conditions which is the substrate arrangement that offer more dispersion of heat during deposition process. Heat disperse easily due to the existence of convection, conduction and radiation of heat transfer concept (Sidebotham, 2015). The middle region results for Micro-Vickers hardness reading average at 191.4648HV are averagely valued between the top and bottom region with top region produce the average hardness reading of 201.0684HV second to bottom region that produce the highest hardness reading of 213.315HV. This may be affected by the substrate arrangement that offer three mediums for the heat to transfer through air, shielding gas and the substrate.

4.5 Microstructural Analysis

Optical microscope shows the microstructure of the surface of welded mild steel under optical microscope using 50x and 100x magnification. Sample 3 was used and analyzed at three different region which is the top, middle and bottom region.

4.5.1 Top Region

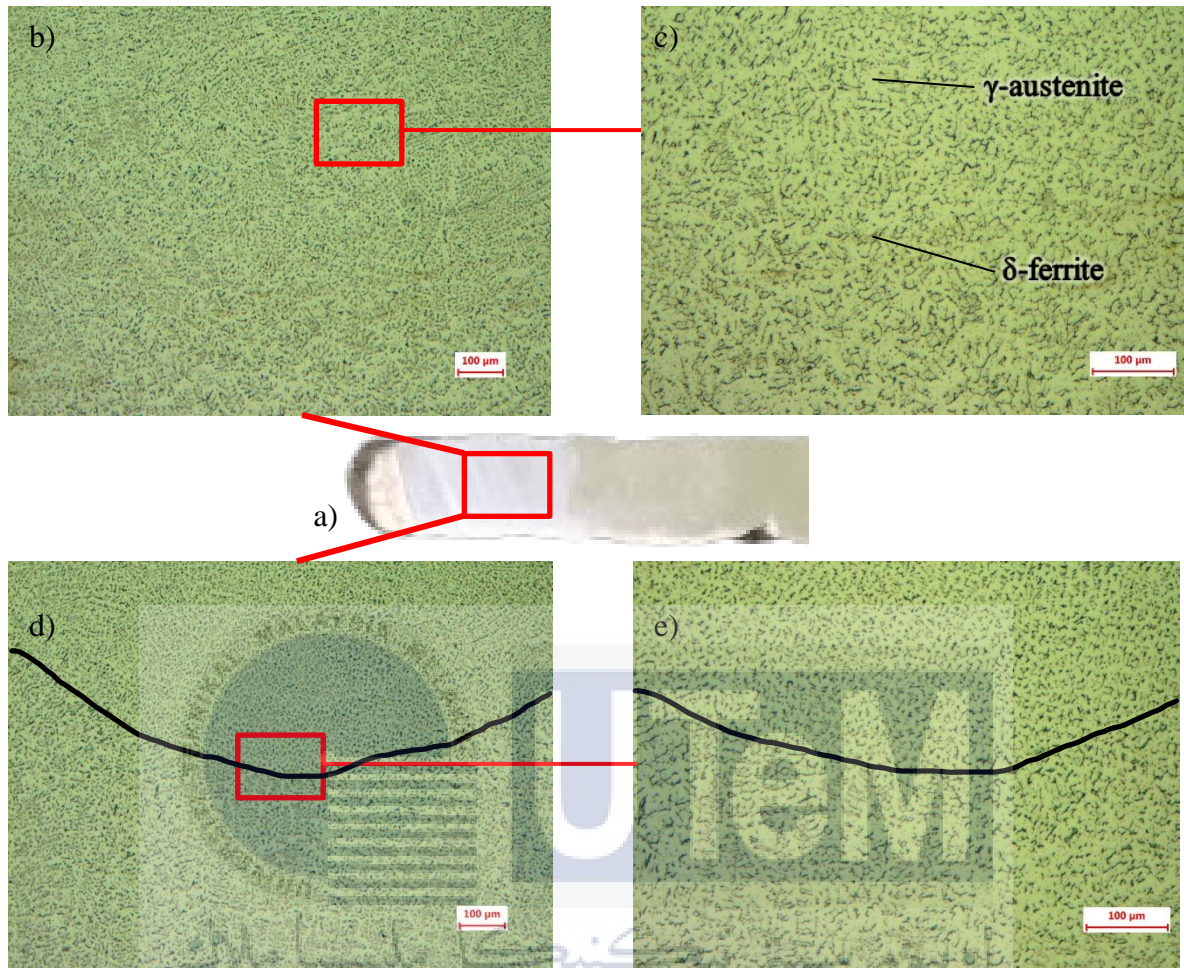


Figure 4.10 a)top region of sample b)microstructure under 50x magnification
c)microstructure under 100x magnification d)layer boundary under 50x magnification
e)layer boundary under 100x magnification

Figure 4.10 c) shows a γ -ferrite arrangement on the top region depict a vermicular pattern. This pattern appears on most of the surface of the top sample. More γ -ferrite means increase in hardness properties thus justify the hardness result in top region.

Figure 4.10 d) shows how more arranged the γ -ferrite arrangement after a new layer. The γ -ferrite on the upper layer shows how more arranged the microstructure compared to the lower layer. This might occur due to the lower layer were introduced to the heat during

the upper layer deposition thus make the lower layer more scattered compared to the upper layer.

4.5.2 Middle Region

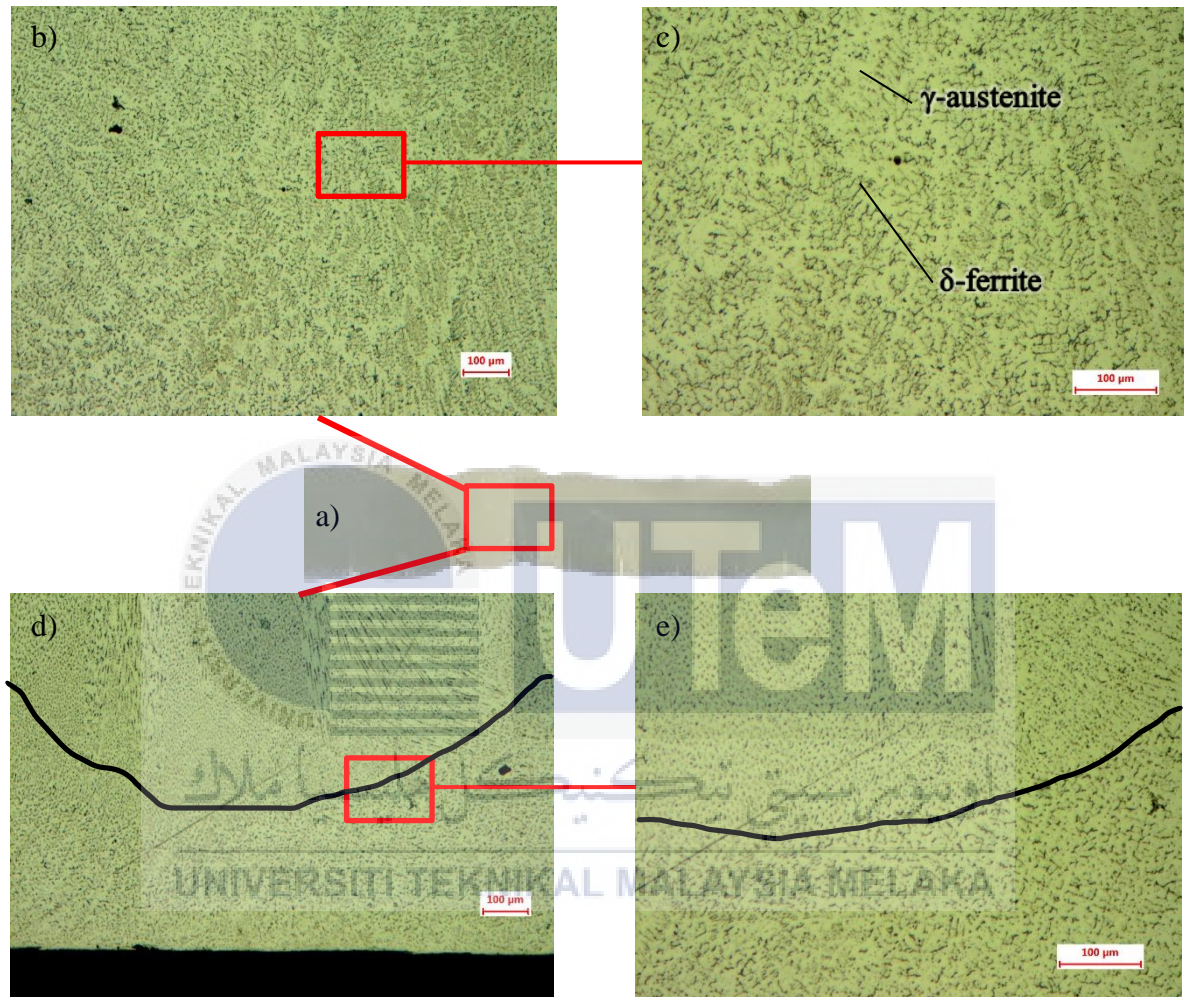


Figure 4.11 a)middle region of sample b)microstructure under 50x magnification
c)microstructure under 100x magnification d)layer boundary under 50x magnification
e)layer boundary under 100x magnification

Figure 4.11 c) shows a δ -ferrite arrangement on the middle region also depict a vermicular pattern but a bit grouped compared to the top region. The γ -austenite in the middle region is clearer compared to the top region thus highlight that it has better ductility compared to the top region. This pattern appears on most of the surface of the middle sample. This indicates that the middle region demonstrates lower hardness compared to the top region thus justify the hardness value in the middle region

Figure 4.11 d) same as the top region, shows how more arranged the δ -ferrite arrangement after a new layer. The δ -ferrite on the upper layer shows how more arranged the microstructure compared to the lower layer but occur some columnar pattern on the upper region. This indicates that the middle region requires more observation and improvement during deposition process be it in welding parameter aspect or heat accumulating aspect.

4.5.3 Bottom Region



Figure 4.12 a)bottom region of sample b)microstructure under 50x magnification
 c)microstructure under 100x magnification d)layer boundary under 50x magnification
 e)layer boundary under 100x magnification

Figure 4.12 c) shows a δ -ferrite arrangement on the bottom region depict a vermicular pattern the same as the top region. This pattern appears on most of the surface of the bottom

sample. The δ -ferrite can be seen more than γ -austenite thus conclude its superiority in hardness compared to the middle region.

Figure 4.12 d) same as the both top and middle region, shows how more arranged the δ -ferrite arrangement after a new layer. The δ -ferrite on the upper layer shows how more arranged the microstructure compared to the lower layer and well more structured compared to the top region. This indicates that the bottom region has the best hardness properties compared to the top region.

4.6 Summary

The tensile test shows that all four sample did produce near isotropy characteristic but a bit variety in deference of both side from each sample. Side B from sample 3 shows the highest tensile stress value at 694.317MPa while the lowest tensile stress value, 601.292MPa, came from Side A from sample 4. Charpy impact test average result does produce isotropy result with small difference between both sides. The highest value of energy absorbed is from side B from sample 2 and side A from sample 3 at 79.88 J while the lowest energy absorbed is from side A from sample 2 at 70.31 J. Micro-Vickers hardness readings fall halfway between those of the top and bottom regions in the middle region. The hardest part is at the bottom, and the softest part is at the middle. The substrate arrangement, which offers three mediums for heat transfer (air, shielding gas, and substrate), is probably what caused this variation. Microstructure analysis found that the δ -ferrite composition in the top and bottom region is more congested compare to the middle region while the middle region shows lower composition of δ -ferrite compared to another region thus justify the hardness result.

5 CHAPTER 5

CONCLUSION AND RECOMMENDATIONS

5.1 Conclusion

The main objective of this experiment was to examine the influence of deposition strategy on the mechanical properties of stainless steel 308Lsi using the MIG robot welding integrated with CMT power source. The evaluation of these properties was conducted using tensile, impact, microhardness and microstructure analysis. The experiment conducted for this project can be concluded successfully accomplished the research objectives. The WAAM sample were successfully built and undergo all testing and analysis and did produce an isotropic characteristic of its mechanical properties.

Analysis of the tensile test revealed that both sides of the sample did produce a different value of young modulus but not quite far from each other. The outcome for both sides still yields a different value for each side when compared to other studies. The maximum load total average at 1.111kN. The difference between both sides produces a tensile strain and tensile stress at maximum load total averaged 0.08 and 30.845 MPa, respectively. Sample 2 showed the most difference in both direction while sample 1 and 3 bring the gap between both sides closer while sample 4 data showed isotropic behavior with just a little difference in young modulus's value. These variations of value may occur due to preparation of specimens such as milling that cause a lot of heat and stress to affect the final result. While some specimens obtained from both sides of a particular WAAM sample exhibited isotropic behavior, others did not. When it comes to tensile stress, side B yields

the highest result at 694.317 MPa while side A's result is 601.292 MPa. It can be concluded, therefore, that isotropy was achieved albeit imperfectly.

On the other hand, the impact test that were focused on the energy absorbed was the main concern. Samples 1 and 4 showed significant isotropy, with a slight difference on both sides. The difference in absorbed energy between samples 1 and 4 was 2.55J and 0.66J, respectively. Samples 2 and 3, on the other hand, revealed a significant variation in the amount of energy absorbed on both sides. The difference in sample 2 was 9.57J, and the difference in sample 3 was 15.67J. Impact testing revealed that, on average, side A, which absorbed the most energy (19.88J), produced better results than side B, which absorbed the least energy (64.21). Value variations in specimens may result from specimen preparation techniques such as milling, which produce heat and stress and affect the final product. In a WAAM sample, certain specimens from both sides exhibited isotropic behavior, while others did not.

In addition, the microstructure analysis reveals that the top and the bottom region of the sample depicts a well-structured vermicular δ -ferrite pattern. The middle region still presents a vermicular δ -ferrite pattern but more grouped and less congested compared to bottom and top region. Suggesting that the bottom and top region offers better mechanical properties. This may occur due to the heat accumulation during deposition process. The bottom region is where the deposition process started thus less heat were accumulated. The top region also accumulated less heat due to heat dispersion through convection through shielding gas, conduction through substrate and radiation through air. The bottom region also accumulated less heat because it was the beginning of the deposition process and less area were covered thus less heat accumulated. The middle region in the other hand accumulated more heat from the bottom and top region during deposition thus explain the microstructure on all three regions.

Lastly, the microhardness test result shows that the hardness value varies as the height increase along the build direction. The bottom region produces the highest hardness value followed with top and last is the middle region. This may be correlated with the microstructure analysis that the well-structured vermicular δ -ferrite pattern on the bottom region and the top region did offer a better result in hardness test compared to the middle region.

5.2 Recommendation

This study suggests several recommendations to improve the result for future studies.

Some of the recommendations are:

- i. During the microhardness result discussion, topic of heat transfer came out to explain the hardness result. The concept of convection, conduction and radiation may exist during the deposition process. In the future, this study may be improved by taking temperature during the deposition process to observed whether this concept really affect the microstructure and mechanical properties result.
- ii. Instead of tilting the work table or the positioner, future studies may suggest tilting the robot nozzle. This matter can be studied whether it can affect the microstructure and the mechanical properties of the WAAM sample.
- iii. Utilize the Scanning Electron Microscopy (SEM) or X-Ray Diffraction (XRD) to dive deeper onto the microstructure aspect and to study the chemical compound of the WAAM sample.
- iv. Integrate alumina powder into WAAM sample during deposition process to observe and study the effect it has.

- v. Produce sample in odds number rather than even amount to smoothen the comparison and average result discussion.

5.3 Project potential

The results of this study could make a big difference in the field of materials engineering and improve printed stainless steel's performance in applications using WAAM. The aim of this study is to investigate significant problems concerning the anisotropic property of stainless steel. This will be accomplished by using a positioner or a tilted work table to give the WAAM sample an isotropic characteristic. Through this research, stainless steel's mechanical qualities and attributes could be improved, which would benefit a variety of engineering applications.

The enhanced mechanical characteristics of printed stainless steel can lead to enhanced stress and strain characteristics, as well as increased hardness and flexibility. The project has the potential to impact economic factors in addition to technical ones. Enhancing the qualities of materials could lead to more cost-effective solutions for sectors that rely significantly on WAAM and stainless-steel components. Overall, the research shows promise in expanding the field of materials engineering and resolving real-world issues pertaining to stainless steel's mechanical attributes.

REFERENCES

- Anand, S., Haldar, N., Datta, S., & Das, A. (2023). Experimental investigation on microstructure and mechanical property of wire arc additively manufactured SS308L built part. *Sadhana - Academy Proceedings in Engineering Sciences*, 48(4).
<https://doi.org/10.1007/s12046-023-02260-7>
- DebRoy, T., Wei, H. L., Zuback, J. S., Mukherjee, T., Elmer, J. W., Milewski, J. O., Beese, A. M., Wilson-Heid, A., De, A., & Zhang, W. (2018). Additive manufacturing of metallic components – Process, structure and properties. *Progress in Materials Science*, 92, 112–224. <https://doi.org/10.1016/j.pmatsci.2017.10.001>
- Derekar, K. S. (2018). A review of wire arc additive manufacturing and advances in wire arc additive manufacturing of aluminium. *Materials Science and Technology (United Kingdom)*, 34(8), 895–916. <https://doi.org/10.1080/02670836.2018.1455012>
- Dickens, P. M., Pridham, M. S., Cobb, R. C., Gibson, I., & Dixon, G. (1992). Rapid prototyping using 3-D welding. *Solid Freeform Fabrication Proceedings*, 280–290. <https://repositories.lib.utexas.edu/handle/2152/64409>
- Gross, A. J., & Bertoldi, K. (2019). Additive Manufacturing of Nanostructures That Are Delicate, Complex, and Smaller than Ever. *Small*, 15(33), 1–6.
<https://doi.org/10.1002/sml.201902370>
- Hadjipantelis, N., Weber, B., Buchanan, C., & Gardner, L. (2022). Description of anisotropic material response of wire and arc additively manufactured thin-walled stainless steel elements. *Thin-Walled Structures*, 171(December 2021).
<https://doi.org/10.1016/j.tws.2021.108634>
- Hassel, T., & Carstensen, T. (2020). Properties and anisotropy behaviour of a nickel base alloy material produced by robot-based wire and arc additive manufacturing. *Welding in the World*, 64(11), 1921–1931. <https://doi.org/10.1007/s40194-020-00971-7>
- Heilig, M. L. (1994). Method of making decorative article. *ACM SIGGRAPH Computer Graphics*, 28(2), 131–134.

- Huang, S. H., Liu, P., Mokasdar, A., & Hou, L. (2013). Additive manufacturing and its societal impact: A literature review. *International Journal of Advanced Manufacturing Technology*, 67(5–8), 1191–1203. <https://doi.org/10.1007/s00170-012-4558-5>
- Ibrahim, I. A., Mohamat, S. A., Amir, A., & Ghalib, A. (2012). The effect of Gas Metal Arc Welding (GMAW) processes on different welding parameters. *Procedia Engineering*, 41(Iris), 1502–1506. <https://doi.org/10.1016/j.proeng.2012.07.342>
- Jafari, D., Vaneker, T. H. J., & Gibson, I. (2021). Wire and arc additive manufacturing: Opportunities and challenges to control the quality and accuracy of manufactured parts. *Materials and Design*, 202, 109471. <https://doi.org/10.1016/j.matdes.2021.109471>
- Jin, W., Zhang, C., Jin, S., Tian, Y., Wellmann, D., & Liu, W. (2020). Wire arc additive manufacturing of stainless steels: A review. *Applied Sciences (Switzerland)*, 10(5), 1–28. <https://doi.org/10.3390/app10051563>
- Khodabakhshi, F., & Gerlich, A. P. (2018). Potentials and strategies of solid-state additive friction-stir manufacturing technology: A critical review. *Journal of Manufacturing Processes*, 36(September), 77–92. <https://doi.org/10.1016/j.jmapro.2018.09.030>
- Liu, W., Jia, C., Guo, M., Gao, J., & Wu, C. (2019). Compulsively constricted WAAM with arc plasma and droplets ejected from a narrow space. *Additive Manufacturing*, 27(March), 109–117. <https://doi.org/10.1016/j.addma.2019.03.003>
- Navarro, M., Matar, A., Diltemiz, S. F., & Eshraghi, M. (2022). Development of a low-cost wire arc additive manufacturing system. *Journal of Manufacturing and Materials Processing*, 6(1). <https://doi.org/10.3390/jmmp6010003>
- Novelino, A. L. B., Carvalho, G. C., & Ziberov, M. (2022). Influence of WAAM-CMT deposition parameters on wall geometry. *Advances in Industrial and Manufacturing Engineering*, 5(May), 100105. <https://doi.org/10.1016/j.aime.2022.100105>
- Ribeiro, F. (1996). Metal Based Rapid Prototyping for More Complex Shapes. *Biennial International Conference on "Computer Technology In Welding*, 1–11. <http://hdl.handle.net/1822/3119>

- Robert, B., & Brown, E. B. (2004). *Assessment of design mechanical parameters and partial safety factors for wire-and-Arc Additive Manufactured stainless steel. 1*, 1–14.
- Shockey, H. K. (1930). Machine for reclaiming worn brake drum. *ACM SIGGRAPH Computer Graphics*, 28(2), 131–134.
- Sidebotham, G. (2015). Heat Transfer Modeling. In *Heat Transfer Modeling*.
<https://doi.org/10.1007/978-3-319-14514-3>
- Singh, S., Sharma, S. K., & Rathod, D. W. (2020). A review on process planning strategies and challenges of WAAM. *Materials Today: Proceedings*, 47, 6564–6575.
<https://doi.org/10.1016/j.matpr.2021.02.632>
- Sun, L., Jiang, F., Huang, R., Yuan, D., Guo, C., & Wang, J. (2020). Anisotropic mechanical properties and deformation behavior of low-carbon high-strength steel component fabricated by wire and arc additive manufacturing. *Materials Science and Engineering: A*, 787(February), 139514. <https://doi.org/10.1016/j.msea.2020.139514>
- Tomar, B., Shiva, S., & Nath, T. (2022). A review on wire arc additive manufacturing: Processing parameters, defects, quality improvement and recent advances. *Materials Today Communications*, 31(May), 103739.
<https://doi.org/10.1016/j.mtcomm.2022.103739>
- Tomaz, I. do V., Colaço, F. H. G., Sarfraz, S., Pimenov, D. Y., Gupta, M. K., & Pintaude, G. (2021). Investigations on quality characteristics in gas tungsten arc welding process using artificial neural network integrated with genetic algorithm. *International Journal of Advanced Manufacturing Technology*, 113(11–12), 3569–3583. <https://doi.org/10.1007/s00170-021-06846-5>
- Ujje, A., & Montanye, A. E. A. (1973). *PROCESS AND APPARATUS FOR TRIPLE-ELECTRODE MIG WELDING USING SHORT-CIRCUIT AND SPRAY-ARC DEPOSITION. 19*.
- Ujje, A. (1966). US3558846A - Method of and apparatus for constructing substantially circular cross section vessel by welding. *Google Patents*.
<https://patents.google.com/patent/US3558846A/en>

- Veiga, F., Suárez, A., Artaza, T., & Aldalur, E. (2022). Effect of the Heat Input on Wire-Arc Additive Manufacturing of Invar 36 Alloy: Microstructure and Mechanical Properties. *Welding in the World*, 66(6), 1081–1091. <https://doi.org/10.1007/s40194-022-01295-4>
- Wohlers, T., & Gornet, T. (2012). History of additive manufacturing Introduction of non-SL systems Introduction of low-cost 3D printers. *Wohlers Report 2012*, 1–23.
- YILMAZ, R., & HUSEYIN UZUN. (2002). Mechanical Properties of Austenitic Stainless Steels. *Journal Of Marmara for Pure and Applied Science*, 10(8), 253–260. <https://doi.org/10.2514/8.11064>
- Yuan, Y., Li, R., Bi, X., Gu, J., & Jiao, C. (2022). Experimental and Numerical Investigation of CMT Wire and Arc Additive Manufacturing of 2205 Duplex Stainless Steel. *Coatings*, 12(12). <https://doi.org/10.3390/coatings12121971>
- Zeng, J., Nie, W., & Li, X. (2021). The influence of heat input on the surface quality of wire and arc additive manufacturing. *Applied Sciences (Switzerland)*, 11(21). <https://doi.org/10.3390/app112110201>
- Zhang, Y. M., Li, P., Chen, Y., & Male, A. T. (2002). Automated system for welding-based rapid prototyping. *Mechatronics*, 12(1), 37–53. [https://doi.org/10.1016/S0957-4158\(00\)00064-7](https://doi.org/10.1016/S0957-4158(00)00064-7)

APPENDICES

Appendix A

Gant Chart for PSM 1

Activities	Status	Week													
		1	2	3	4	5	6	7	8	9	10	11	12	13	14
Title registration with supervisor	Plan														
	Actual														
Project explanation from supervisor	Plan														
	Actual														
Defining problem statement, objective and project scope	Plan														
	Actual														
Drafting & writing chapter 1	Plan														
	Actual														
Material preparation	Plan														
	Actual														
Defining & finding reference for literature review	Plan														
	Actual														
Drafting & writing chapter 2	Plan														
	Actual														
Defining methodology on research	Plan														
	Actual														
Drafting & writing chapter 3	Plan														
	Actual														
Revising chapter 1, 2, 3, preliminary result before submission	Plan														
	Actual														

Gant Chart for PSM 2

Activities	Status	Week (Semester 7)													
		1	2	3	4	5	6	7	8	9	10	11	12	13	14
PSM 2 implementation	Plan	■													
	Actual	■													
Discussion with supervisor	Plan	■	■	■											
	Actual		■	■											
Method used for experiment	Plan			■	■	■									
	Actual			■	■	■									
Experiment setup	Plan	■	■	■	■										
	Actual			■	■	■	■								
Material and equipment selection and supervisor meeting	Plan			■	■	■	■	■							
	Actual			■	■	■	■	■							
Experiments and testings	Plan			■	■	■	■	■	■	■					
	Actual			■	■	■	■	■	■	■					
Listing all results	Plan										■	■	■		
	Actual										■	■	■		
Writing chapter 4	Plan								■	■	■	■			
	Actual								■	■	■	■			
Writing chapter 5	Plan									■	■	■	■		
	Actual									■	■	■	■		
Report checked by supervisor	Plan													■	■
	Actual													■	■